INFORMATION TO USERS

This reproduction was made from a copy of a manuscript sent to us for publication and microfilming. While the most advanced technology has been used to photograph and reproduce this manuscript, the quality of the reproduction is heavily dependent upon the quality of the material submitted. Pages in any manuscript may have indistinct print. In all cases the best available copy has been filmed.

The following explanation of techniques is provided to help clarify notations which may appear on this reproduction.

1. Manuscripts may not always be complete. When it is not possible to obtain missing pages, a note appears to indicate this.

2. When copyrighted materials are removed from the manuscript, a note appears to indicate this.

3. Oversize materials (maps, drawings, and charts) are photographed by sectioning the original, beginning at the upper left hand corner and continuing from left to right in equal sections with small overlaps. Each oversize page is also filmed as one exposure and is available, for an additional charge, as a standard 35mm slide or in black and white paper format.*

4. Most photographs reproduce acceptably on positive microfilm or microfiche but lack clarity on xerographic copies made from the microfilm. For an additional charge, all photographs are available in black and white standard 35mm slide format.*

***For more information about black and white slides or enlarged paper reproductions, please contact the Dissertations Customer Services Department.**

U·M·I Dissertation Information Service

University Microfilms International
A Bell & Howell Information Company
300 N. Zeeb Road, Ann Arbor, Michigan 48106

Khazbak, Atef

CORRELATED WAVE FUNCTION CALCULATIONS OF THE CHEMISORPTION OF WATER ON A CLEAN TITANIUM (0001) SURFACE

City University of New York PH.D. 1986

PLEASE NOTE:

In all cases this material has been filmed in the best possible way from the available copy. Problems encountered with this document have been identified here with a check mark __✓__.

1. Glossy photographs or pages _____
2. Colored illustrations, paper or print _____
3. Photographs with dark background _____
4. Illustrations are poor copy _____
5. Pages with black marks, not original copy _____
6. Print shows through as there is text on both sides of page _____
7. Indistinct, broken or small print on several pages ✓
8. Print exceeds margin requirements _____
9. Tightly bound copy with print lost in spine _____
10. Computer printout pages with indistinct print _____
11. Page(s) _____ lacking when material received, and not available from school or author.
12. Page(s) _____ seem to be missing in numbering only as text follows.
13. Two pages numbered _____. Text follows.
14. Curling and wrinkled pages _____
15. Dissertation contains pages with print at a slant, filmed as received _____
16. Other _____

_____

_____

University
Microfilms
International

CORRELATED WAVE FUNCTION CALCULATIONS OF THE CHEMISORPTION OF WATER ON A CLEAN Ti (0001) SURFACE

by

ATEF KHAZBAK

A dissertation submitted to the Graduate Faculty in Physics in partial fulfillment of the requirements for the degree of Doctor of Philosophy, The City University of New York.

1986

This manuscript has been read and accepted for the Graduate Faculty in Physics in satisfaction of the dissertation requirement for the degree of Doctor of Philosophy.

Date

Professor C.R. Fischer C.R. Fischer
Chairman of Examining Committee

Date

Professor Joel Gersten Joel Gersten
Executive Officer

Professor J. Marion Dickey

Professor Jacob Neuberger

Professor Ann Marie Sapse

Professor Thomas Venanzi

Supervisory Committee

The City University of New York

ABSTRACT

CORRELATED WAVE FUNCTION CALCULATIONS OF THE CHEMISORPTION OF WATER ON A CLEAN Ti (0001) SURFACE

by

Atef Khazbak

Advisor: Professor C.R. Fischer

The Hartree-Fock-Roothaan Self-Consistent-Field (SCF) Method supplemented by configuration interaction (CI) was used to study the interaction and dissociation of a water molecule on a Titanium surface. The calculations were made tractable by using a Ti core potential and by a unitary localization transformation to define a local surface region of localized lattice plus adsorbate orbitals for the CI calculations. Three Ti clusters were considered Ti_3, Ti_7 and Ti_{28}. The dissociated H_2O (OH + H) was found to be bound on the three clusters with binding energy ranging from 25 K cal/mol to 36 K cal/mol. The 3 d electrons were shown to play a limited role in bonding and to create an activation barrier for molecular H_2O as it approaches the surface. The completely dissociated H_2O (O + 2H) was found to be unbound indicating that atomic oxygen derived from H_2O does not exist on the surface.

ACKNOWLEDGEMENTS

I would like to express my gratitude to Professor C. Rutherford Fischer for providing me with the opportunity to finish this work. His guidance, contributions and assistance is highly appreciated.

I am indebted to Professor J.L. Whitten of Stony Brook University for his useful suggestions and to Mrs. Susan Wasserman for typing this manuscript and her help.

TABLE OF CONTENTS

LIST OF TABLES

LIST OF ILLUSTRATIONS

CHAPTER I

INTRODUCTION

I.1 Chemisorption and Physical Adsorption

When a gas molecule approaches the surface of a solid, it might interact in two different ways. The weaker interaction (Van der Waals), is due to the correlation of the movement of electrons; it is a physical adsorption and does not involve sharing of electrons between the adsorbate and the surface. The stronger interaction or chemisorption, which involves sharing of electrons, usually occurs at a smaller distance from the surface.

Since gas molecules move freely in three dimensions and since adsorbed molecules are, at best, restricted to two dimensional motion, the adsorption process is accompanied by a decrease in entropy ΔS. Further, the change in free energy ΔG must be negative for adsorption to take place. Use of the equation

$$\Delta H = \Delta G + T\Delta S \qquad (I.1)$$

shows that ΔH, the heat of adsorption, is bound to be negative. The conclusion is that all adsorption processes are exothermic.

There are certain differences in the properties of the two kinds of adsorption, which can be used as criteria for deciding the adsorption type.

(i) The best single criterion is the magnitude of heat of adsorption. Chemical bonds are normally stronger than physical forces of attraction, and the heat of chemisorption should therefore be higher. Heats of chemisorption vary widely between 15 and 200

K cal/mole, whereas heats of physical adsorption are all in the range 2 - 15 K cal/mole.

(ii) Chemisorption, being a chemical reaction, may require an appreciable activation energy. In this case it will only proceed at a reasonable rate above a certain minimum temperature. Physical adsorption on the other hand requires no activation energy. It should therefore be exceedingly rapid at any temperature.

(iii) Chemisorption possesses a certain specificity which physical adsorption does not. This is partly because it depends upon the adsorbent being clean, partly because not all surfaces, even when clean, are active in chemisorption. Physical adsorption on the other hand takes place on all surfaces under the correct conditions of temperature and pressure.

(iv) The chemical saturation of a surface is usually satisfied by chemisorption of a single layer. With physical adsorption no such limitation applies.

A chemisorptive bond does not differ in principle from ordinary chemical bonds, and is due to the same electrostatic forces which operate in atoms and molecules. The only special feature of the chemisorptive bond is that it can, depending on the circumstances, be composed of highly delocalized molecular orbitals, a situation which is seldom encountered in ordinary chemical bonds.

I.2 Localized and Non-Localized Adsorption

A surface may be represented diagrammatically as a plane, the potential energy of which fluctuates from point to point. When these fluctuations are appreciable the troughs represent adsorption sites, and adsorption is therefore said to be localized. If, however, the fluctuations are so small as effectively to vanish, there are no adsorption sites, and adsorption is said to be non-localized.

Chemisorption is always localized, and in localized adsorption two extreme conditions may be distinguished. If the energy fluctuation is the same between any pair of sites and all sites have the same energy, the surface is said to be uniform or homogeneous. If the fluctuation is irregular and the sites have different energies, the surface is said to be non-uniform or heterogeneous. Examples of the two types of surface are shown in Fig.I.1. Since homogeneous and heterogeneous surfaces have very different properties in adsorption and catalysis, it is important to know to which of these classes a given surface belongs.

In non-localized adsorption there is no energy barrier opposing movement of a particle from point to point on the surface, while in localized adsorption there is a barrier. Therefore, with non-localized layers, the kinetic thermal energy of the adsorbed particles is sufficient to ensure that they will be mobile and move over the surface, but localized layers may be mobile or immobile, according as the thermal energy is greater or less than the energy barrier between sites. With localized adsorption, mobility reduces to a series of migrations from site to site each requiring an activation energy. On a uniform surface, this energy will be the same for each migration, but on a

non-uniform surface it will be different.

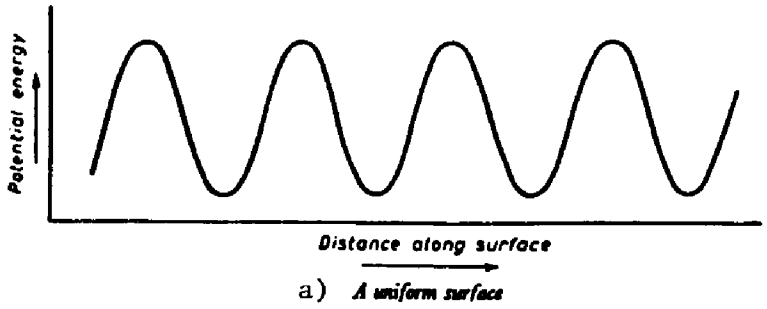

a) *A uniform surface*

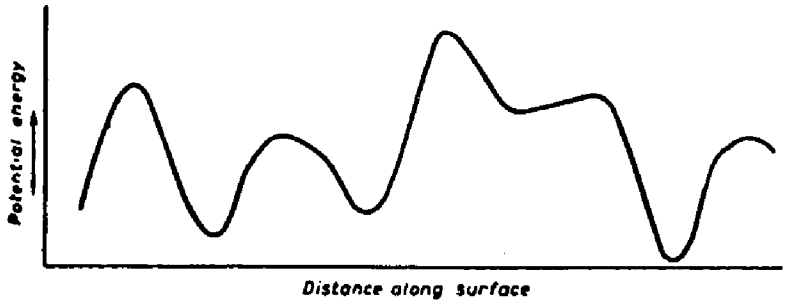

b) *A non-uniform surface*

Figure I.1 Potential energy for a) A uniform surface

b) A non-uniform surface

I.3 Cluster Chemisorption

I.3.1 Background

In the past several years, considerable emphasis has been placed on the study of solid surfaces and on the interaction of adsorbates with such surfaces. This interest has arisen for a number of reasons. The most important of these are: surface problems are of considerable scientific and technical interest in and of themselves; the sensitivity of experimental procedures, and the power of theoretical techniques combined with the increased availability of high-speed digital computers have finally made possible surface science studies to a wide variety of investigators. An example of a problem of considerable scientific as well as technological interest concerns the influence of surface defects on chemisorption. The other paramount reason for the interest in surface science has been brought about by the "energy crisis". Considerable interest has been focused on the use of more efficient catalysts for coal gasification, or fuel cells for example, or producing better converters for solar generation of electricity. The net result of all this has been an enormous effort in understanding the various properties of solids.

I.3.2 Choice of the Problem

The cluster by virtue of its finite physical size is from the outset clearly unsuited to describe any physical phenomenon for which the spatial extent of that phenomenon is greater than the physical extent of the cluster in any significant way. On this basis, a study of phenomenona involving say, electrical conductivity or the energy bands of a metal would require a cluster so large as to be impractical

from the computational standpoint. Such long-range phenomena are better studied using the techniques of energy band theory. On the other hand, phenomena which have a physical extent smaller than the spatial extent of the cluster may be ideal subjects for a cluster simulation.

Chemisorption and the formation of chemical bonds is amenable to study by cluster techniques for several reasons. These include the fact that chemical bonds are normally regarded as being of short range in character (typically of order one internuclear separation) and therefore a cluster large than the bond length is easily studied. In many real world cases the adsorbate during chemisorption is not deposited in a uniform ordered layer on a surface and hence long-range order in the plane of the surface is absent. Traditional solid state techniques using translational periodicity are of little use, and here a cluster model is useful and efficient. Therefore for those problems in which long range order does not occur naturally, cluster models are preferable.

I.4 Chemisorption on d-Band Metals

There is more experimental data on the surface of transition metals than on any other class of solid surfaces. The reasons primarily are that their surfaces are relatively easy to clean and they are very important technologically. With the recent advent of angular photoemission, experiment is well ahead of theory in studies of the surface electronic structure of these metals.

The electronic structure of d-band metals is a field apart from that of the simple metals. They are more complex and of course more interesting than the simple metals; if their electronic structure is complicated, that of their surfaces is more so, and their chemisorptive properties far more so still.

These difficulties arise from the unique character of the d-electrons themselves, whose intermediate nature is not shared by any other entity in the whole periodic table. In general electrons in solids may be easily divided into core electrons and valence or bonding electrons. The core electrons are tightly bound to their nuclei and are little affected by the presence of other atoms in the solid. They are so well localized near the nucleus that they essentially do not overlap the electrons of other atoms and do not notice their presence. In most calculations they are easily and routinely ignored, or orthogonalized out of the problem or frozen.

The valence electrons behave just the opposite. They overlap so strongly from one atom to another as to lose any real identification with any specific atom. As a consequence, it becomes a good description to treat them as free-running plane waves traversing the whole system.

This desirable situation deteriorates in the case of d-electrons. Their wave functions have maxima well inside the atom and decay rapidly further out; what is more, the changes in the central region of the atom on putting the atom into a solid are perceptible but small. Clearly this is rather core-electron-like behavior. However the tail of the d-electron wave functions extend a long way out; the tails on neighboring atoms overlap considerably and are modified on going from isolated atom to solid. This is valence electron behavior.

This intermediate behavior complicates matters and what is even worse is that most d-band metals are characterized by a partially filled d shells; the extent of that filling changes between atom and solid, and requires some kind of self consistent calculation to get the correct occupancy. For the surface case, further charge rearrangement is expected, making self-consistency even more important. And finally chemisorption, the subject of this thesis, introduces the severest problem in allowing charge transfer between substrate and adsorbate.

A considerable number of calculations of chemisorption of gas molecules at transition metal surfaces has been carried out in the past few years. For example Bagus and Seel calculated properties of chemisorption of Co on Cu[1], and Goddard and co-workers considered Co on Ni[2]. Fischer, Burke and Whitten[3] have studied the chemisorption of Co on Ti. In the present work we are considering the chemisorption of a water molecule on Ti (0001) surface using the Hartree-Fock Roothaan SCF-CI Method.

I.5 Methods of Obtaining a Solution

Methods used for cluster studies fall into two basic types, empirical methods and nonempirical methods. Within each method there is a plenty of subdivisions. The empirical methods, which are sometimes refered to as semiempirical methods, make use of the experimental data, and are at their best qualitative. Depending on the parametrization, they can give interesting results. However, due to the simplicity of the models, studies involving excited states, unpaired electrons and correlation effects are not possible. Examples of these methods are the Extended Huckel Model (EHT)[4] and the X_α Method[5]. Within the category of nonempirical methods, also often termed ab initio or first principle method, one can further subdivide into two general categories, variationally determined models, such as Hartree-Fock, and local density models which have a conceptual basis in the Hohenberg-Kohn Theorem[6].

I.6 Ab Initio Molecular Orbital Studies

An ab initio self-consistent field MO method is defined in this work as an approximate Hartree-Fock treatment in which all of the interactions are treated explicitly and calculated rigorously.

I.6.1 Outline of the Theory

An ab initio molecular orbital calculations usually consists of three steps. The first step is the computation of overlap, kinetic, nuclear attraction and electron repulsion integrals. In the second step these integrals are used to construct the Fock matrix which is diagonalized to obtain the SCF wave functions. The third step, the inclusion of electron correlation effects, is usually carried out by configuration interaction calculations.

Since the number of Fock matrix elements increases as the square of the number of electrons, each of these steps becomes unmanageable in a chemisorption study involving a lattice with more than about twenty to thirty atoms. One of the techniques used is to assume that a limited number of orbitals actively participate in bonding with an adsorbed species. Then one can exclude the remaining lattice orbitals from an explicit variational calculation.

The excluded orbitals are the core orbitals of the metal atoms which are not likely to be important in mixing with valence orbitals. A well known approximation is to replace the field of the core orbitals by a local pseudopotential. The second class of invariant orbitals is singled out after doing an exchange maximization localization in the immediate vicinity of the adsorption site. These orbitals shows a minimum exchange interactions with the adsorption site and are frozen in the core of the final CI step. This procedure reduces the number

of molecular orbitals appearing explicitly in the transformation and also limits the configuration interaction space.

1.6.2 SCF-CI Method

The SCF-CI method starts with the usual Restricted Hartree-Fock-Roothan SCF[7,8] formulation to describe the transition metal cluster plus adsorbate. Since the size of the Fock matrix depends on the number of the variationally determined orbitals, the atomic core orbitals of the transition metal are not varied, but their interaction with the valence orbitals are accounted for accurately. That is, the atomic core electrons of the metal are assumed to be localized, but give rise to coulomb and exchange potentials which are accurately evaluated along with contributions due to core-valence orbital overlap. This is usually handled by constructing a pseudopotential for the valence electrons. Following Whitten and Pakkanen[9], the valence basis functions of a given atom are rigorously orthogonalized to the core orbitals of the atom using a simple auxiliary basis. The Gram-Schmidt orthogonalization method is applied to introduce the core orbitals into the valence space. For the adsorbate, all the orbitals are treated as valence orbitals and are involved in the entire SCF calculation.

I.6.3 Localization on the Active Chemisorption Site

Consider a system described by a single determinant wave function, for the N valence electrons

$$\Psi = A(\Phi_1, \Phi_2, \ldots \Phi_N) \qquad (I.2)$$

A is the usual anti-symmetrizing operator.

There are N_α and N_β spin orbitals $\{\Phi_K\}$. Suppose this system is to interact with a second system $\{\chi_K\}$, where $\{\chi_K\}$ are the atomic orbitals of the designated chemisorption site. The set $\{\Phi_K\}$ is now transformed by applying a unitary transformation to obtain a new set $\{\Phi'_K\}$. For the new set to interact strongly with the atomic orbitals of the designated chemisorption site, the sum of the exchange integrals is maximized.

$$\gamma = \sum_{k=1}^{M} [\chi_K(1)\ \Phi'(1)|\ \frac{1}{r_{12}}|\ \chi_K(2)\ \Phi'(2)] \geq 0 \qquad (I.3)$$

where $\Phi' = \sum_i c_i \Phi_i$

and M is the number of the atomic valence orbitals of the chemisorption site. This leads to an eigenvalue problem with solutions, ordered in eigenvalues $\gamma_1 \geq \gamma_2 \geq \ldots \gamma_N$

$$\begin{aligned}
&\gamma_1 && \Phi'_1 = \sum_i C_{i1} \Phi_i \\
&\gamma_2 && \Phi'_2 = \sum_i C_{i2} \Phi_i \\
&\gamma_p && \Phi'_p \\
&\gamma_{p+1} && \Phi'_{p+1} \\
&\gamma_N && \Phi'_N = \sum_i C_{iN} \Phi_i
\end{aligned} \qquad (I.4)$$

The total wave function

$$\Psi = A(\Phi'_1, \Phi'_2, \ldots \Phi'_N) \qquad (I.5)$$

is identical to the initial wave function of equation I.2. After some member γ_p in the eigenvalue spectrum, the orbitals $\Phi'_{p+1}, \ldots \Phi'_N$ exhibit negligible exchange interaction with the orbitals $\{\chi_K\}$. The new functions $(\Phi'_1, \Phi'_2 \ldots \Phi'_p)$ represents localized molecular orbitals on the designated atoms, bonds between these atoms, and bonds linking the designated atoms with the remainder of the lattice. It does not follow that all orbitals $\{\Phi'_i\}$, $i \leq p$, will be localized only over one or two atoms, and tails into the lattice which are in part a consequence of orthogonality will occur.

Similarly, it is also of interest to carry out a localization transformation within the virtual space since the resulting localized orbitals are those orbitals primarily needed for configuration interaction refinement of the local region.

It should be noted that it is the existence of a dual orbital space, one associated with designated atoms, and one associated with the lattice wave function, that distinguishes the present localization scheme from Ruedenberg exchange maximization method[10]. Since the set $\{\chi_K\}$ is invariant, the present localization calculation is not iterative.

The occupied transformed orbitals $\Phi'_{p+1}, \ldots \Phi'_N$ which have small amplitudes in the local region are referred to as interior orbitals, and are used as the core orbitals in the final CI step, while those defining the local region are the localized occupied orbitals $\Phi'_1, \Phi'_2, \ldots \Phi'_p$ and the localized virtual orbitals $\Phi''_1, \Phi''_2, \ldots \Phi''_q$. The

local region is thus best defined as a p-electron subspace localized around a designated surface site; it can not be equated to the set of atoms used to generate the localization, nor to any particular set of atoms near the site of interest.

In summary, the objective of this localization scheme is to define an interior part of the lattice electron distribution which can be taken as invariant during the course of interaction with the adsorbate and to introduce the important delocalization characteristics of an extended lattice into the concept of a local region near the surface.

I.6.4 Configuration Interaction Treatment of the Adsorbate-Surface Interactions

It is evident that a proper account of electron correlation is required to achieve an accurate description of the following phenomena: the energetics of interaction, the vibrational frequency of the incoming molecule, bond breaking and formation processes, and the electronic response of the lattice to the incoming adsorbate. The most elementary purpose of configuration interaction is to allow variable ionic and covalent character, and to ensure proper dissociation limits and description of weak bonds. The existence of closely spaced single particle states in a cluster of metal atoms leads to a large number of electronic states near the ground state. Thus, the ground state can be highly degenerate, and the only satisfactory way to proceed is to allow nearly degenerate electronic configurations to enter by allowing a direct mixing of configurations.

The N electron wave function for a given electronic state Ψ_k is formulated as a linear combination of configurations Ψ_ℓ

$$\Psi_k = \sum_\ell C_{k\ell} \Psi_\ell \qquad (I.6)$$

where configurations are constructed from orthonormal molecular orbitals obtained by promoting electrons from ground state SCF orbitals. A set of doubly occupied orbitals with low lying ground state orbital energies, called the fixed core is chosen to be common to each of the ground and excited configurations. Wave functions and energies are generated by a multistep procedure. The initial wave functions $\{\Psi^1_j\}$, for the M electronic states of interest are expressed as linear com-

binations of the configurations $\{\Phi_k^1\}$, which are expected to be important contributors to at least one of the M states,

$$\Psi_j^1 = \sum_k C_{kj}\Phi^1{}_k \quad j = 1, 2 \ldots M \tag{I.7}$$

Additional configurations, $\{\Phi_k^2\}$, are then generated analytically by performing single or double promotions from the initial set of configurations $\{\Phi_k^1\}$ subject to

$$\frac{|\langle\Phi_k^2|\ H\ |\ \Phi_j^1\rangle|^2}{|\langle\Phi_k^2|\ H\ |\ \Phi_k^2\rangle - \langle\Psi_j^1\ |H|\ \Psi_j^1\rangle|} > \delta \tag{I.8}$$

for at least one j = 1, 2, ... M, where $\delta = 10^{-2} - 10^{-3}$ a.u., and H is the fixed nuclei electrostatic Hamiltonian

$$H = \sum_i [-\frac{1}{2}\nabla_i^2 - \sum_k Z_k r_{ik}^{-1}] + \sum_{i<j} r_{ij}^{-1} \tag{I.9}$$

The new set of configurations $\{\Phi_k^2\}$ is combined with the inital set $\{\Phi_k^1\}$, and improved CI wave functions,

$$\Psi_j = \sum_{i=1}^{2} \sum_k C_{k_j}{}^i \Phi_k^i , \quad j = 1, 2, \ldots M$$

and energies E_j are calculated by diagonalization of the Hamiltonian matrix.

The lowest energy CI wave functions are defined as the parent set Ψ_j^1 and the entire process is repeated one or more times using the improved CI wave functions, with $\delta = 10^{-4} - 10^{-5}$ a.u. typically, until convergence is achieved for the states of interest. At each step of the procedure, the set of configurations is augmented to contain all

configurations necessary to assure that the total wave function is an eigen function of S^2. An approximate, successive diagonalization method described in reference 11 is used for the diagonalization of the large matrices that occur in the final steps of the CI process.

CHAPTER II

THERMODYNAMICS AND EXPERIMENTAL TECHNIQUES

II.1 Thermodynamics

II.1.1 Introduction

A gas atom or molecule feels an attractive potential upon approaching surfaces of different kinds. The strength of this potential determines the nature of the interaction between the gas and the surface atoms. The strength of the interaction can be expressed in terms of experimentally measurable parameters in several ways. An important parameter, which describes the interaction is the heat of adsorption ΔH. It is the average binding energy per mole between the interacting gas atoms and surface atoms and is related to the depth of the potential energy well.

For $\Delta H >> RT$, where RT is the average thermal energy associated with one mole of gas atoms, the atoms undergo strong interaction with the surface which results in partial or total energy transfer and adsorption. For $\Delta H \simeq RT$ the adsorption probability is small. However, if this condition is obtained by raising the surface temperature to produce high thermal energy to match the large interaction energy, strong interaction and complete energy transfer can still take place. This is indicated by the dissociation of gas molecules on hot metal surfaces. If the condition $\Delta H \simeq RT$ is obtained on account of the shallow well depth of the interaction potential, there will be no appreciable energy transfer and weak interaction will take place.

The temperature range of study distinguishes experimentally weak physical adsorption from strong adsorption. Adsorption studies for weakly interacting systems have to be carried out at low temperature. For chemisorption, large surface concentrations of the adsorbed gas can be secured even at temperature higher thatn 300°K, because of the large attractive interaction potential between the surface and gas atoms.

Once the gas atom is adsorbed, the ratio of the well depth of the interaction potential ΔH and the thermal energy of the gas atoms at the surface, $\Delta H/RT$, also determines the residence time of the gas atom on the surface. Measurement of the residence time can also give one an estimate of the type of interaction that takes place between the gas and the surface. Weak interactions implies smaller residence time.

II.1.2 Adsorption Isotherms

Most of the information about the nature of the adsorbed gas layer comes from macroscopic studies of the amount of gas adsorbed on the surface σ, surface coverage, as a function of gas pressure p at a given temperature. The σ - p curves are called adsorption isotherms. The adsorption isotherms are used to determine thermodynamic parameters that characterize the adsorbed layer (heats of adsorption, entropy and heat capacity changes associated with the adsorption process) and to determine the surface area of the adsorbing solid.

In most chemisorption processes the heat of adsorption is thought to decrease with coverage because of the repulsive interaction between adsorbate molecules when they are in close proximity to each other. Let us assume that the heat of chemisorption decreases as a linear func-

tion of the coverage, which can be expressed as

$$\Delta H = \Delta H_o(1 - a\theta) \qquad \text{(II.1)}$$

where ΔH_o is the heat of chemisorption at zero coverage, a is a proportionality constant, and θ is often called the degree of covering and is written as

$$\theta = \frac{\sigma}{\sigma_o} \qquad \text{(II.2)}$$

If σ_o is the surface coverage in the completely covered surface, the number of surface sites available for adsorption, after adsorping σ molecules, is $\sigma_o - \sigma$. Of the total flux F incident on the surface, a fraction $\frac{\sigma}{\sigma_o} F$ will strike molecules already adsorbed and therefore be reflected. Thus a fraction $(1 - \frac{\sigma}{\sigma_o})F$ of the total incident flux will be available for adsorption, so we can write

$$\sigma = (1 - \frac{\sigma}{\sigma_o}) F\tau \qquad \text{(II.3)}$$

where τ is the residence time

$$\tau = \tau_o \exp\ (\frac{\Delta H}{RT}) \qquad \text{(II.4)}$$

The gas flux F is proportional to the pressure and from the kinetic theory of gasses could be written as,

$$F = \frac{N_o P}{\sqrt{2\pi MRT}} \qquad \text{(II.5)}$$

M is the molecular weight, P is the pressure. Using II.2, equation II.3 could be written as

$$\frac{\theta}{1-\theta} = \frac{1}{\sigma_o} F\tau \qquad \text{(II.6)}$$

or

$$\frac{\theta}{1-\theta} = AP \exp\left[\frac{\Delta H}{RT}\right] \qquad \text{(II.7)}$$

where $A = N_o(2\pi MRT)^{-\frac{1}{2}} \tau_o \sigma_o^{-1}$

or, using equation II.1

$$\frac{\theta}{1-\theta} = AP \exp\left[\frac{\Delta H_o(1-a\theta)}{RT}\right] \qquad \text{(II.8)}$$

or, in logarithmic form after rearrangement.

$$\text{Ln } p = \text{Ln } \frac{\theta}{1-\theta} - \text{Ln } A_o + \frac{\Delta H_o a\theta}{RT} \qquad \text{(II.9)}$$

where $A_o = A \exp[\Delta H_o/RT]$ is independent of coverage. In the range $0.1 < \theta < 0.9$ which is most accessible to chemisorption experiments, the term $\text{Ln}[\theta/(1-\theta)]$ varies very slowly with coverage. For chemisorptiom characterized by a strong interaction potential, $\Delta H >> RT$, the third term on the right side dominates. Thus, we can write

$$\theta \approx \frac{RT}{\Delta H_o a} \text{Ln } A_o P \qquad \text{(II.10)}$$

This isotherm, which predicts the linear variation of θ with Ln p, is the Temkin isotherm[12]. In the middle range of surface coverage, this isotherm accurately describes the chemisorption of many gases.

II.2 Experimental Techniques for Surface Structure

In recent years a number of methods have come into use that provide information about the structure of a solid surface, its composition, and the oxidation state present. In essentially all cases the solid-high vacuum interface is probed with a beam of ions, electrons or electromagnetic radiation, and various diffraction, scattering and other atomic processes are observed. In no case can a good description of the properties of the chemisorptive system be obtained using a single experimental technique; the combined use of various methods is necessary. Several approaches to obtain structural information have been attempted. Low energy electron diffraction (LEED) intensity analysis has proved to be a powerful method for determining the locations of adsorbed atoms. Spectral resolution of orbitals of adsorved species may be obtained by using photo-electron-spectroscopy, mainly with UV sources (UPS).

II.2.1 Low Energy Electron Diffraction (LEED)

II.2.1.1 Background

It was recognized very early in the history of diffraction studies that just as x-rays and relatively high energy electrons (say 50 KeV) gave information about the bulk periodicity of a crystal, low energy electrons (around 100 eV) whose penetrating power is only a few atomic diameters, should give information about the surface structure of the solid. The first reported experiment is that of Davisson and Germer[13] in 1927, with marginal results. Work was handicapped by considerable experimental difficulties in generating a beam of monoenergetic electrons, in detecting its scattering, and, even more by

the fact that at that time ultrahigh vacuum techniques had not been developed. Even at pressure of 10^{-6} torr (mm Hg) a surface becomes covered with a monolayer of adsorbed gas in about 1 second. To be sure of dealing with clean surfaces, pressures down to 10^{-10} torr are needed.

II.2.1.2 Diffraction Condition

Consider a wave incident on a crystal surface, with an amplitude A in free space at a given point r

$$A(r) = A(o) \exp [i(Kr - \omega t)] \qquad (II.11)$$

Here A(o) is the amplitude at an arbitrary origin, r = 0, and K is the wave vector of the travelling wave which has an angular frequency ω. The magnitude of K is given by $|K| = \frac{2\pi}{\lambda}$, where λ is the wave length associated with the motion of the electrons, according to De Broglie

$$\lambda = \frac{h}{mv} = \frac{h}{(2mE)^{\frac{1}{2}}}$$

or

$$\lambda(A^\circ) = \frac{12}{[E(eV)]^{\frac{1}{2}}} \qquad (II.12)$$

For a given K, it can be shown that the electrons are scattered by a periodic three dimensional lattice only in well-defined directions corresponding to wave vectors satisfying the conditions

$$\vec{K}' = \vec{K} + \vec{G} \qquad (II.13)$$

where $\vec{K}'$ is the wave of the scattered beam. Diffraction can occur only if the magnitude of the incident and scattered wave vectors

remain the same, $|\vec{K}'| = |\vec{K}|$. This is the case of elastic scattering in which the incident electrons suffer no energy loss. A typical diffraction condition is shown in Fig. II.1. The spacing, d, between lattice planes (h, k, ℓ) of the crystal is given by

$$d(h\ k\ \ell) = \frac{2\pi}{|\vec{G}(h\ k\ \ell)|} \qquad \text{(II.14)}$$

Thus the magnitude of any reciprocal lattice vector $|G(h\,k\,\ell)|$ is

$$|\vec{G}(h\,k\,\ell)| = \frac{2\,\pi\,n}{d(h\,k\,\ell)} \qquad \text{(II.15)}$$

and from Figure II.1 we can see that

$$|\vec{G}(h\,k\,\ell)| = |\Delta\vec{K}| = 2\,|\vec{K}|\sin\theta$$

Then

$$\frac{2\,\pi\,n}{d(h\,k\,\ell)} = 2\,|\vec{K}|\,\sin\theta$$

where θ is the half-angle between the scattering vectors $\vec{K}$ and $\vec{K}'$. Since $|\vec{K}| = \frac{2\pi}{\lambda}$, we have arrived at the Bragg reflection law

$$2\ d\ \sin\theta = n\ \lambda$$

For LEED the wave vector $\vec{K}$ in units of A^{o-1} is defined by the electron beam energy as

$$K = \frac{2\pi}{\lambda} = 0.512\ [E(eV)]^{\frac{1}{2}}$$

For x-ray diffraction, the scattering cross section is small; therefore the incident beam intensity is much larger than the intensity

of the scattered beam. Thus the probability of double scattering is small. For LEED, where the scattering cross sections are large, the amplitudes of the various diffracted beams can be of the same order of magnitude as the amplitude of the incident electron beam. So double diffracting or, in general, multiple-scattering of low energy electrons may also take place. The experimental verification of the importance of double diffraction and other multiple-scattering events in LEED comes from studies of curves of the intensity versus electron energy.

II.2.1.3 LEED Apparatus

A low energy electron diffraction apparatus is in principle one of the simplest electron optical devices (as compared e.g. with the high performance transmission electron microscope). A parallel beam of electrons having an energy from a few tens to a few hundreds of electron volts impinges on a crystal and is back diffracted in directions given by the well known Ewald construction. Diffracted electrons are registered either on a fluorescent screen or by measurement of their current with a Faraday collector. The arrangement of LEED equipment is influenced by the nature of LEED, because apart from the elastically reflected electrons there are electrons reflected from the sample with a loss of energy. They contain no diffraction information and cause a background intensity which makes it difficult to observe the diffraction spots. It is therefore necessary to filter out electrons having a lower energy than the primary one. However, these electrons could be used in other experiments to measure electron binding energies in the different energy states for surface atoms (Auger spectroscopy).

II.2.1.4 LEED, Catalysis and Chemisorption

Catalysis denotes the acceleration of a chemical reaction by means of a substance which is not consumed during the reaction. In heterogenous catalysis the reaction is accelerated by interaction between the reactants and a solid surface. The important step in this speeding up process occurs in the adsorbed state at the surface. Characterization of ordered adsorbed phases by means of LEED is there-

fore vital to the understanding of the mechanism, particularly where more than one reactant is involved. The various stages in a catalytic process can be observed by the changes in the LEED pattern.

Since heterogenous catalysis involves processes in the adsorbed state one is primarily interested in the answers to the following questions:

1) What is the configuration of an adsorbed particle with respect to the surface atoms of the catalyst?
2) What configurations have the adsorbed particles relative to each other?

Question (1) is strongly connected to the theory of the chemisorption bond, whereas (2) is related to the interaction between the adsorbed particles and can be treated theoretically by statistical methods. It is evident that the two problems are closely related to each other. In general there will exist an optimum arrangment of a single adsorbed particle with respect to the surface atoms, and at the same time, for a given coverage, a most favorable configuration of the adsorbed particles relative to each other. Optimum correlations for both types of interactions will probably not occur together and thus the two will compete in the determination of the final surface structure.

For periodic structures the positions of diffraction spots in the reciprocal lattice is determined only by the geometry of the elementary cell, whereas the intensity depends on the dynamic scattering factors. As a consequence question (2) may be answered immediately in those cases where the primitive cell contains only one adsorbed particle.

However, an answer to question (1) from LEED information can be achieved in only a few special cases where additional arguments are available.

Owing to the statistical behavior of the system the arrangement of the adsorbed particles is not perfectly periodic. If the periodic regions are relatively small the diffraction spots are broadened and vice versa. From the spot diameter the size of ordered domains can be estimated. With anisotropic surfaces this size may depend on the orientation and this may cause elongated spots or streaks in the diffraction pattern[14]. It is also possible to devise the symmetry of the adsorption sites from the type of spot broadening[15]. The progress of surface processes can be followed from variations of the position, shape, or intensity of diffraction spots with time.

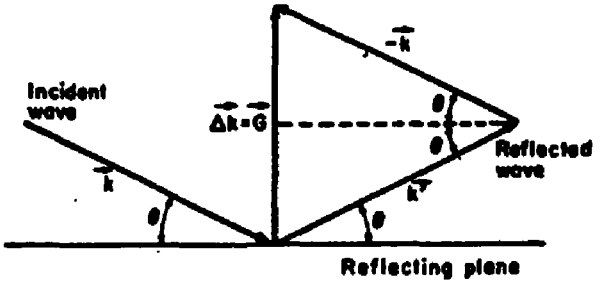

Figure II-1. *Determination of* $\Delta \mathbf{k} = \mathbf{k}' - \mathbf{k}$ *in terms of the angle of scattering* θ.

II.2.2 Ultraviolet Photoemission Spectroscopy (UPS)

II.2.2.1 Introduction

When a photon beam with an energy between 6 and 100 eV or high energy electromagnetic radiation is allowed to strike a solid surface, in addition to electron emission from the valence band, electrons are excited from inner electron shells as well. The two primary inner-shell excitations are shown in Fig. II.2. The notation used is the one most commonly used in atomic spectroscopy: the K, L, M, ... shells refer to those with principal quantum number n = 1, 2, 3, ... , with K, L_I, L_{II}, L_{III} refer to $1s_{1/2}$, $2s_{1/2}$, $2p_{1/2}$, $2p_{3/2}$ respectively.

An electron may be ejected from the K shell into vacuum. If the energy of the incident radiation is greater than the binding energy of the electron, this process, which is commonly called photoelectron emission can take place. From the knowledge of the incident beam energy and by suitable analysis of the ejected photoelectrons, the electronic binding energies in the different bands can be obtained. On the other hand, the electrons may only be excited into the conduction band of an insulator or just above the Fermi level in a metal, and in this case the energy of excitation is adsorbed by the atoms. By variation of the energy of the incident beam, the adsorption spectrum characteristics of a given solid can be obtained, and from the adsorption peaks at different energies, the electronic binding energies can again be determined.

Energy analysis of the emitted photoelectrons is called photoelectron spectroscopy, and the energy analysis of the absorption peaks is called x-ray absorption spectroscopy. In general, the photoelectron spectra give peaks of better energy resolution than the absorption

spectra.

In the study of chemisorption one is only interested in the surface bonding states with binding energy less than 10 eV below the Fermi energy. Therefore ultraviolet photons of energy between 5 and 100 eV are suitable for this study.

II.2.2.2 UPS Apparatus and Data Analysis

A monochromatic ultraviolet photon beam is incident on the sample, which is prepared in an ultra-high-vacuum chamber, and is the source of the ejected photoelectrons. The emitted electrons are detected by the detector and energy analyzed by the energy analyzer together with associated electronics for recording energy distributions. The energy of the ejected photoelectrons E depends on the incident photon energy E_{photon} and is given by

$$E = E_{photon} - E_b - \Phi_a \qquad \text{(II.17)}$$

where E_b is the electron binding energy in the shell from which it is ejected and Φ_a is the work function of the analyzer. The electronic binding energy is calculated using Eq. II. 17.

Fig. II.3 shows a typical photoelectron spectrum. The intensity of the peaks can be used to determine relative or absolute concentrations of the different elements. In addition to the detection of elemental chemical composition, photoelectron spectroscopy can distinguish between the different oxidation states of elements, because of a shift in the binding energies of inner-shell electrons upon the change of valency. By monitoring these chemical shifts, photoelectron spectroscopy has not only been able to distinguish between different oxidation states but

also to detect other changes in the chemical environment that lead to the distribution of the electron density. The UPS study is expected to answer the following questions:

1) What is the density of states of the chemisorbed system?
2) What is the binding energy of each state in the chemisorbed system?
3) What is the chemical shift of the new chemisorbed system relative to the old system?

Combining the results of LEED, UPS and other experimental techniques (atomic and molecular beam scattering, change of work function during adsorption, Auger electron spectroscopy) a consistent physical picture of chemisorption seems to emerge.

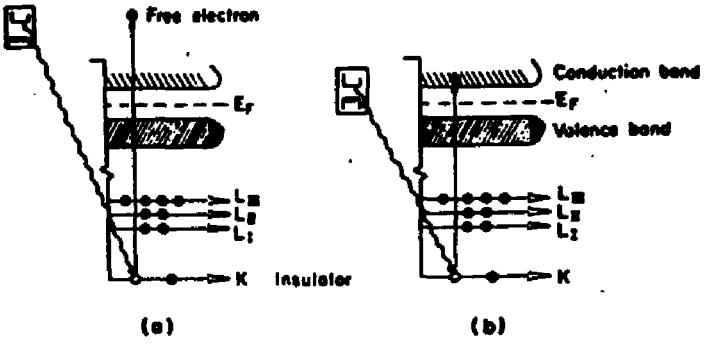

Figure II-2. *Energy-level-diagram representation of (a) photoelectron emission and (b) x-ray absorption.*

Figure taken from reference 16, p. 175.

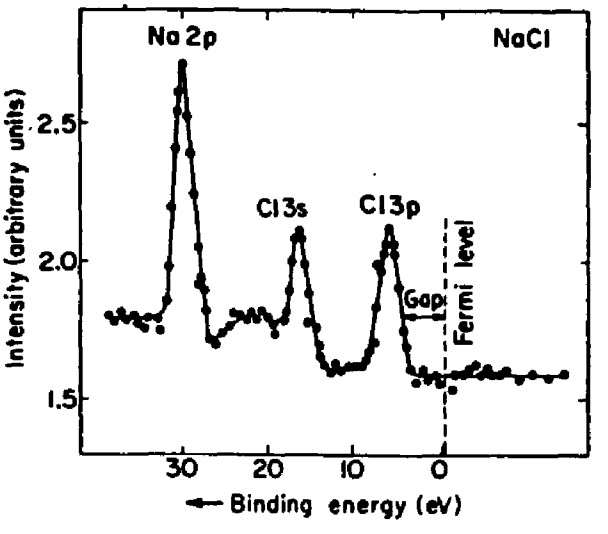

Figure II-3. ***Photoelectron spectrum of sodium chloride.***

Figure taken from reference 16, p. 182.

CHAPTER III

Correlated Wave Function Calculation of the Chemisorption of Water on Ti (0001)

III.1 Introduction

Water adsorbed on various substrates has been the subject of a number of recent experimental studies. This is due in part to the importance of adsorbed water in a variety of chemical processes such as heterogenerous catalysis, electrolysis, and formation of aerosols on metal particulates. These experiments have shown that water undergoes several possible reactions on a metal surfaces involving either dissociation or molecular adsorption. Early Ultraviolet Photoemission Spectroscopy (UPS) studies of Atkinson et al[17] suggested that water adsorbed on Mo dissociates. Fisher, Gland and Sexton[18] determined that OH was formed on Pt (111) when water was co-adsorbed with oxygen at low temperature and allowed to warm up. They observed a Pt-O-H scissors vibration in electron-energy-loss spectroscopy (EELS). Also using EELS, Ibach and Lehwald[19] saw evidence for free OH and H after adsorption of H_2O on Pt (100). Water was found to react strongly with FE (001) by Dwyer et al[20] using low energy electron diffraction and Auger electron spectroscopy (AES).

Benndrof et al[21], with the use of UPS, saw evidence for molecular H_2O adsorption on Ni (110) at low temperature followed by the formation of an ice overlayer at high coverages. Recently; Rosenberg et al[22] have studied the photon stimulated desorption (PSD) of ions from amorphous ice. The only ion species they observed in the photon energy 20 - 30 eV was H^+. Netzer and Madey[23] in their study of the electron-

stimulated desorption (ESD) of H_2O on Ni (111) found the dominant ion to be H^+, which indicates a dissociation process.

At present photoemission[24, 25] and electron-energy-loss spectroscopy[26-28] (EELS) have come to opposite conclusions about whether the H_2O molecule stays intact or dissociates into H and OH on a silicon surface. In the photoemission spectra three H_2O - induced valence orbitals are observed and have been assigned to chemisorbed molecular H_2O. It has been concluded that the molecule is adsorbed with the oxygen end down, which results in the observed bonding shift of the oxygen lone-pair molecular orbitals. On the other hand in all EELS studies on the H_2O - Si system, the observed losses are assigned to Si-H, Si-OH and SiO-H vibrations and it is concluded that water is dissociated on silicon surfaces. The adsorption of H_2O on CU (100) and Pd (100) at temperature around 10 K has been investigated by Anderson et al[29] using EELS and water is found to adsorb associatively as monomers at low converages with its molecular axis significantly tilted relative to the surface normal.

Müller and Harris[30] used the Kohn-Sham scheme to calculate the interaction energy of an H_2O monomer with cluster simulating different adsorption sites on an Al (100) surface. A well defined atop-atom ground state with the molecular plane tilted away from the normal is found. The adsorption is accompanied by a substantial donation of charge to the metal. The binding energy is 0.53 eV. Recently Ribarsky et al[31] considered the interaction of H_2O with a Cu (100) surface via cluster calculations using the self-consistent-field-linear-combination-of-atomic orbitals-Xα method. In the equilibrium on-top configuration

bonding is found to be through the oxygen with the molecular plane tilted from the normal. Bonding involves the H_2O lone-pair orbitals and a charge donation to the metal. The ground state binding energies determined via systematic mappings of the potential energy surfaces are E_B (H_2O - Cu) = 0.76 eV and E_B (H_2O - Cu_5) = .38 eV.

In the present study we consider the theoretical treatment of the adsorption and dissociation of a single water molecule on a Ti (0001) surface using an electronic theory that permits the accurate computation of molecule solid surface interaction, The SCF-CI theory is based on a many electron approach in which the configuration interaction follows an ab initio self consistent field calculations on an adsorbate plus surface region. The following objectives are set

A) Calculations on a small cluster H_2O-Ti_3 to determine preliminary information about the system including the role of the s and d electrons in bonding.

B) Calculations of selected adsorption sites on the seven atom "surface" hexagonal cluster.

III.2 Ultraviolet Photoemission Spectroscopy (UPS) of the Interaction of Water with Ti (0001) Surface

Stockbauer et al[32] used UPS to study the adsorption of H_2O on a stepped Ti (0001) crystal. The spectra are shown in Fig. III.1 for adsorption at room temperature (~300K). At a photon energy of 23 eV, a 1.3 eV binding energy feature appears fully resolved from the Ti 3d valence band (curves b and c). At a photon energy of 50 eV, the cross section of the 1.3 eV peak appears to increase relative to that of the valence peak and the photon-energy resolution degreades to such an extent that the peaks are no longer resolved (curves d and e). This feature is identical in form and photon-energy dependence to the 1.3 eV binding energy peak observed when this same crystal was dosed with hydrogen[33]. It has been identified by Feibelman et al[34] as a H-induced surface state on Ti (0001). A broad peak near 6 eV observed in the hydrogen-adsorption experiments was obscured in the H_2O experiment by other peaks in the spectrum. A comparison of the relative intensities of the peaks at 6 and 1.3 eV in the H_2O and the H spectra shows that the intensity of the 6 eV peak in the H_2O spectra is a factor of two higher than in the H spectra, indicating an additional contribution to the 6 eV peak in the H_2O spectra. This contribution is assumed to be from atomic oxygen[35].

The peaks at 7.4 and 11.4 eV BE are ascribed to OH based on their similarity to the peaks observed by Fisher, Gland and Sexton[18] in UPS of oxygen and water coadsorption on Pt (111). A comparison is made with the UPS spectrum of gaseous OH radical which exhibits two dominant features with ionization potentials of 13.0 and 15.2 eV[36].

The location of the gaseous peaks are indicated by the lines above curve d in Fig. III.1, aligned by matching the energy of the gas phase peak of higher ionization potential with the surface OH peak at 11.4 eV. The energy spacings of gaseous and surface OH are different, presumably due to bonding of OH to the Ti surface. The UPS data show no evidence for molecular H_2O on the surface at room temperature.

Fig. III.2 shows the UPS spectra at low temperature (~90 K). At low coverage the same features are observed as the room temperature spectra. Again peaks are noted for H at 1.3 eV, for O at 6 eV, and for OH at 7.4 and 11.4 eV BE. As in the room temperature spectra H_2O appears to be fully dissociated.

At higher coverages, additional features appear: peaks at 8 and 14 eV and a plateau between 9 and 13 eV BE. Their similarity to peaks observed at low temperature by Brundle and Roberts[37] from H_2O on Au, by Fisher, Gland and Sexton[18] from H_2O on Ni (110) leads one to assign these features to molecular H_2O on Ti (0001) surface.

For comparison the room temperature UPS data of CO on Ti (0001) is shown in the curbe f of Fig. III.1 The peaks near 4 and 6 eV BE are due to atomic carbon and oxygen respectively[38]. At low temperature (90 K) CO does adsorb molecularly producing additional peaks at 7.3 and 11.5 eV BE (curve b of Fig. III.2). However the photon energy dependence of the cross section of these two peaks is different from the 7.4 and 11.4 eV peaks in the H_2O adsorption experiments. Based on this evidence, these two peaks are due to the formation of OH when H_2O is adsorbed on Ti (0001) and not due to impurity CO adsorbed on the surface.

The photon stimulated desorption (PSD) shows that the ions desorbed from H_2O-dosed Ti (0001) to be almost H^+ which indicates that OH must be present on the surface in order to produce the measure H^+ signal.

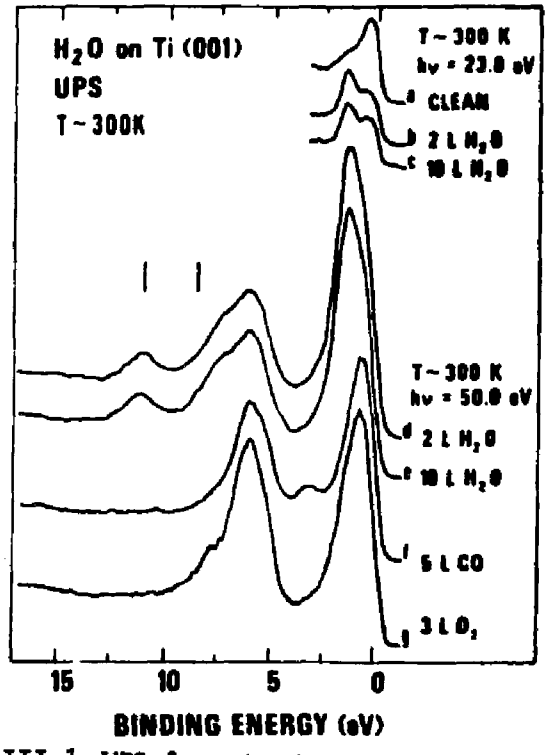

Fig. III.1 UPS of water (*a* – *e*) at room temperature compared with CO (*f*) and O_2 (*g*). Curves *a* – *c* show H-induced surface state. The positions of the OH gas-phase PES peaks (Ref. 17) are shown above curve *d*.

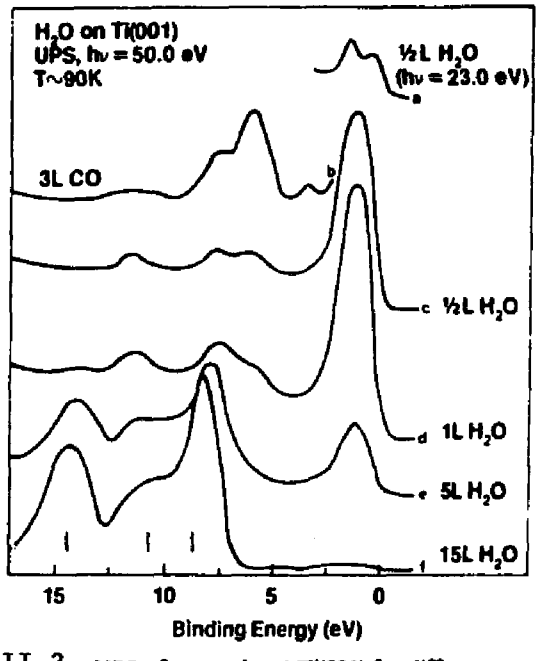

Fig. III.2 UPS of water-dosed Ti(001) for different coverages at ~90 K compared with CO (*b*). Low coverage (*c*) shows only H, O, and OH. At higher coverages (*d* – *f*), peaks corresponding to molecular water appear. The energy of the H_2O gas-phase PES peaks are shown below curve *f*.

III.3 Free H_2O Molecule Calculation

The free H_2O molecule calculation was carried out to check the validity of the hydrogen and oxygen basis functions and to find the orbital and total energy of the free molecule. This total energy plus the energy of the clean lattice serves as a reference for calculating the binding energies of our system.

All atomic core electrons of the oxygen atom are explicitly included. All 10 electrons in the H_2O molecule are involved in the entire SCF calculations. The valence basis was chosen to be 1s, 1s' on each hydrogen atom and 1s, 1s', 2s, 2s', $2p_x$, $2p_x'$, $2p_y$, $2p_y'$, $2p_z$ and $2p_z'$ on the oxygen atom. Gaussian expansions of atomic orbitals are used throughout (see appendix). Fig. III.3 shows the equilibrium geometry for the H_2O molecule. The parameters were taken from Snyder and Basch[39]. Table III.1 shows the orbital and total energy of H_2O together with the Mulliken populations. The charge on each hydrogen atom is 0.72 electron and on the oxygen atom is 8.56 electrons. This confirms the fact that the water molecule is polar with its dipole moment pointing from the oxygen atom to the midpoint of the two hydrogen atoms.

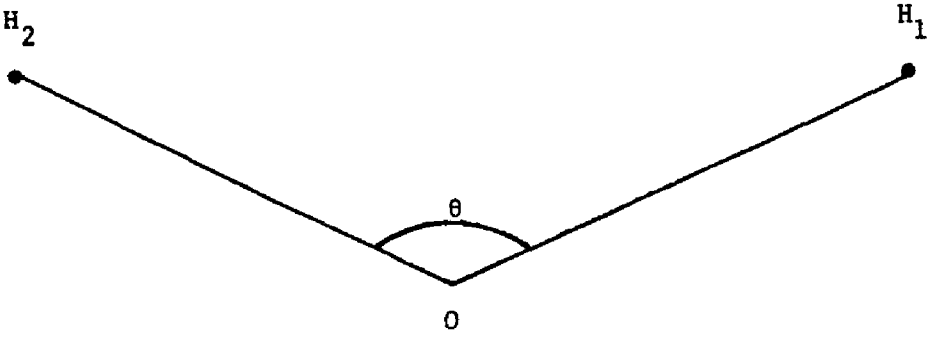

Fig. III.3 Equilibrium Geometry for H_2O Molecule

O-H = 1.8089 A.U.

θ = 104.52°

Table III.1 Total and orbital energies of water

Symmetry of orbital	Orbital energy in a.u.	
$1a_1$	-20.559[a]	-20.558[b]
$2a_1$	-1.363	-1.352
$1b_2$	-0.719	-0.719
$3a_1$	-0.570	-0.582
$1b_1$	-0.510	-0.506
E_{SCF}	-75.989	-76.0593
ΔE_{CI}	-0.118	
E_{Total}	-76.107	

Mulliken population (a.u.)

H_1	0.720
H_2	0.720
O	8.560
H_2O	10.0

a) Present Calculation

b) Taken from D. Neumann and J.W. Moskowitz, J. Chem. Phys. 49, 2056, 1968.

III.4 Electronic Configuration of Titanium

The M-shell (n = 3) of an atom contains three sub-shells, 3s, 3p, 3d. From atomic theory it is known that an orbital wave function with lower angular momentum will tend to penetrate further into the nucleus. This leads to the expected order of occupation 3s, 3p and 3d. However a new phenomenon appears in this M shell. This is because the screening effect due to the inner shells of electrons is gradually diminished by the effective charge of the nucleus with increasing atomic number . In addition, the energy of the state depends on the total quantum number n by a factor of $1/n^2$. These two factors make the energy difference between successive outer shells smaller and smaller. On the other hand, the effects of greater penetration toward the nucleus, by the lower angular momentum state are becoming larger and larger. There is a point then, at which the low angular momentum states of the next higher shell may have a lower energy than the higher angular momentum states of the given shell. This "cross over" first occurs for the 3d subshell and the 4s subshell. The two electrons in the 3d subshell have higher energy than those of the two electrons in the 4s subshell for a titanium atom. However, these four electrons are treated as valence electrons in most chemisorption studies involving titanium.

For bulk titanium, there is some evidence that the configuration is $(3d)^3\ (4s)^1$ compared with $(4s)^2\ (3d)^2$ for the titanium atom[9]. The configuration $(3d)^3\ (4s)^1$ has been applied in the ab initio SCF calculations even though in these calculations a cluster was used to represent a bulk. The size of a titanium cluster which will behave more or less

like a bulk is not known. Bulk titanium is a non-magnetic material while the titanium atom has a net spin of one. Titanium was chosen in the present study to minimize the uncertainties in the theoretical treatment of transition metals. Intrashell correlation for the d electrons is expected to be less important in titanium than, for example in nickel.

III.5 Role of the 3 d and 4 s Electrons in Bonding on Transition Metals

Melius et al[40] have studied the dissociation of H_2 on Ni using multiconfigurational self-consistent field methods. According to their analysis the d electrons remain localized and do not participate directly in bonding; however the d orbitals can serve as a source or reservoir for the valence σ electrons as the state or geometry varies. Kunz and co-workers[41] used the generalized valence-bond and unrestricted Hartree-Fock calculations to study the interaction of S , Mn and Cu with hydrogen. They reported a limited role for the d electrons in bonding. Cremaschi and Whitten[42] have considered the chemisorption of H_2 on Ti (0001) with use of an ab initio SCF-CI method. Their conclusion was that the bonding is predominantly with the 4 s electrons.

Subsequent to the studies of chemisorption by Ni cited above, Messmer et al[43] using the Xα - method have considered the interaction of atomic hydrogen with small clusters of Ni, Pb and Pt. In these studies, one finds strikingly different behavior for the case of Ni-H bonding as compared to Pd-H or Pt-H bonding. In these studies the Ni-H bond is essentially 4 s derived, the Ni-3d contribution being only 35% of the bonding orbital, whereas, the Pd-H bond or the Pt-H bond is mostly metal d in character. Clearly this Xα - study found greater 3 d participation of the bonding of H to Ni than is found by Melius et al[40] who found 3 d participation in the bonding orbital to be less than 20%. A question arises here. Is the greatest d participation in the Xα-model indicative of a significant difference between the Xα

model and the Hartree-Fock like methods or is it due to the different geometries studied? At present this question is unanswered and it would be useful to further study this question.

Fischer and Whitten[44] studied the interaction between Ti and a H atom and between Ti atoms in chains of length two, five and ten by using the Xα-SW method. Their calculation confirmed a significant d participation in bonding. However, their calculation raises some uncertainties mainly due to the rapid increase in intersphere volume as the chain length increases. Also the role of the effect of the constant potential on the d orbitals needs a more detailed investigation.

III.6 Choice of the Cluster

A reasonable choice for the structure of a cluster is to assume a highly symmetrical one and to assume internuclear distances close to the bulk values. The fragments to be considered are those derived from the hexagonal close-packed structure which is the experimentally determined structure for titanium below 820°C. The calculations are performed at the titanium metal internuclear distance of 2.95A^{o}.

The clusters to be considered are the three atom equilateral traingle and the seven atom "surface" hexagonal cluster (Ti_7). Fig. III.4 shows the geometry for these two clusters.

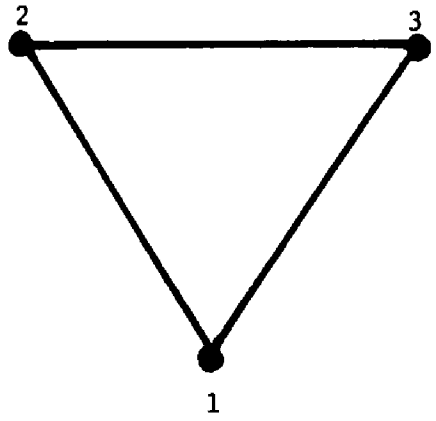

(a) Ti_3

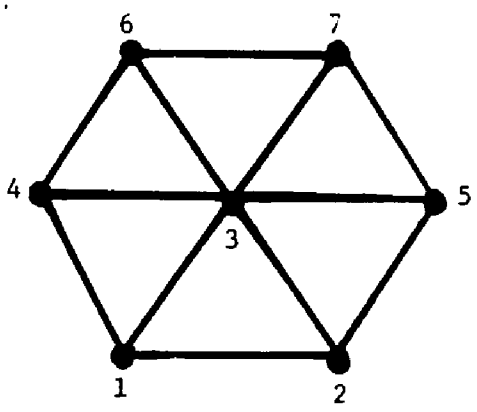

(b) Ti_7

Figure III.4 The two titanium clusters

III.7 Small Cluster Calculation $Ti_3 - H_2O$

III.7.1 Calculation With the 3 d Electrons Assigned to Core

In the present calculation the three electrons in the 3 d orbitals of each Ti atom were assigned to the core together with the ($1s^2$, $2s^2$, $2p^6$, $3s^2$, $3p^6$) electrons and contribute only an electrostatic potential. All the three Ti atoms have the same set of valence basis orbitals, 4s and 4s' (see appendix). The total number of valence electrons in the present system is thirteen since each Ti atom contributes one 4 s electron and the water molecule contributes all its ten electrons. A reasonable choice for the geometry is to consider a highly symmetrical case, with the oxygen atom above the three fold site. In order to decide which way the two hydrogen atoms are pointing on adsorption, two different calculations were done, one with the two hydrogen pointing up away from the lattice, and the other with the two hydrogen pointing down toward the lattice. In both cases the oxygen atom was at 3 a.u. above the three-fold site and the parameters for water molecule are those of the free molecule. Table III.2 shows the results for these two cases. The case with the hydrogen pointing up has lower energy than the sum of the energies of the separated systems and has a binding energy of 0.015 a.u. (0.41 eV), while the case with hydrogen pointing down has higher energy than the sum of the energies of the separated sytems and therefore is unbound (binding energy is negative). Also shown is the Mulliken population analysis for the charge distribution. As we can see the charge transfer between the lattice and the H_2O molecule is greater for the bound state than that for the unbound state.

The UPS experiment has shown that water is adsorbed dissociatively on Ti (0001) surface, and according to our previous results we are encouraged to stretch one of the O - H bonds for the case where the hydrogen is pointing away from the lattice. Table III.3 shows the results for such cases where both SCF and CI calculations are performed. Two important features are noted here (i) As we stretch the O - H_2 bond from 1.8089 a.u. (unstretched) to O - H_2 = ∞, the binding energy goes from the negative value of -0.00018 a.u. (unbound) to the positive value of +0.04 a.u. (bound). The result confirms the fact that H_2O dissociates on the Ti (0001) surface to form H and OH. (ii) The second point to note is that the amount of charge transferred from the lattice to the molecule increases from 0.08 electron for the molecular case to 0.77 electron for the dissociated case.

	H_2O and clean surface (infinite separation)	Hydrogen pointing up	Hydrogen pointing down
E_{SCF} (a.u.)	-76.353 (-75.989-0.364)	-76.368	-76.229
E_B (a.u.)	———	+0.015	-0.124
Mulliken population (a.u.)			
H_1	0.720	0.701	0.713
H_2	0.720	0.701	0.713
O	8.562	8.683	8.53
H_2O	10.0	10.085	9.956
Ti_3	3.0	2.916	3.044
Q_{Total}	13.0	13.0	13.0

Table III.2 Results for the unstretched H_2O on Ti_3. The 3 $\underline{d}$ electrons are assigned to the core orbitals. A positive value for E_B indicates a bound state.

	H_2O & clean surface	OH_2 = 1.8089 a.u.	OH_2 = 2.4 a.u.	OH_2 = 3 a.u.	OH_2 = ∞
E_{SCF} (a.u.)	-76.353	-76.368	-76.373	-76.380	-76.383
E_B (a.u.)	——	+0.015	+0.020	+0.027	+0.020
AE(CI)	-0.118	-0.103	-0.101	-0.108	-0.129
E_{Total} (a.u.)	-76.471	-76.471	-76.474	-76.488	-76.511
E_B (a.u.)	——	0.000	+0.003	+0.017	+0.040 (25.0 $\frac{K\ cal}{mol}$)
Mulliken population (a.u.)					
H_1	0.720	0.701	0.614	0.629	0.641
H_2	0.720	0.701	1.285	1.258	1.0
O	8.562	8.683	8.885	8.975	9.129
H_2O	10.0	10.085	10.784	10.862	OH = 9.77
Ti_3	3.0	2.916	2.217	2.141	2.232
Q_{Total}	13.0	13.0	13.0	13.0	13.0

Table III.3 Results for the stretched H_2O on Ti_3 with hydrogen pointing away from the lattice. The 3 $\underline{d}$ electrons are assigned to the core.

III.7.2 Calculations with the 3 d Electrons Assigned to Valence Orbitals

III.7.2.1 H_2O Molecular Plane is Perpendicular to Lattice Plane

The $(3d)^3$ $(4s)^1$ electronic configuration for titanium has been widely employed in ab initio SCF calculations[9], and in order to decide the role of 3 d electrons in bonding with the adsorbed H_2O molecule we are going to treat the three electrons in the 3 d orbitals as valence electrons. Only the $1s^2$, $2s^2$, $2p^6$, $3s^2$ and $3p^6$ electrons of each Ti atom are assigned to the core and contribute only an electrostatic potential. The three Ti atoms have the same set of valence basis functions $3d_{xy}$, $3d_{xz}$, $3d_{yz}$, $3d_{y^2-z^2}$, $3d_{x^2-z^2}$, 4s and 4s'. Each Ti atom contributes four valence electrons to the system (one 4s and three 3d). The total number of valence electrons in the present system is 22 electrons. Calculations were performed at the SCF level for the two cases where the two hydrogens are pointing up away from the lattice, and pointing down toward the lattice with the oxygen atom at 3 a.u. above the three fold site. The results are shown in table III.4. They are similar to the case in which the 3 d electrons were assigned to the core (Table III.2), i.e., the geometry with the two hydrogens pointing down toward the lattice is very repulsive relative to other geometry. Since the case with the hydrogen pointing up away from the lattice was still slightly repulsive, an SCF followed by CI calculations was done by stretching one of the O-H bonds till complete dissociation occurred. By looking at table III.5, it is seen that the total energy of our system decreases as we stretch the O-H bond from its unstretched value, and the case at which complete dissociation occurs is the most deeply bound state with binding energy of

29.4 K cal/mol. This result confirms the experimental results that H_2O dissociates on the titanium surface to form OH and H. However, by comparing this value of 29.4 K cal/mol binding energy with the value of 25.0 K cal/mol binding energy which was obtained by assigning the three 3d electrons to the core, we can conclude that the 3d electrons play a limited role in the dissociation of H_2O on the titanium surface. This role could be seen through the 3d → 4s promotion of electrons. For the separated systems there are 7.9 d electrons and 4.1 s electrons, while for the dissociated case of H_2O into OH and H there are 7.0 d electrons and 4.3 s electrons.

In order to test the possibility for the dissociation of OH into O and H, another SCF calculation was done by stretching the remaining OH bond. The results of our calculation are shown in table III.6. As we can see, the continuous stretch of the bond causes the energy to go up, and the binding energy becomes more and more negative (unbound state), and the completely dissociated case is the most unbound (binding energy is -0.17 a.u.). This highly repulsive value of binding energy shows that it is not necessary to carry out the CI calculation.

	H_2O + Clean Surface (infinite separation)	Hydrogen Pointing Up	Hydrogen Pointing Down
E_{SCF} a.u.	-85.522 (-75.989 - 9.533)	-85.505	-85.333
E_B a.u.	------	-0.017	-0.189
Q (a.u.)			
H_1	0.720	0.736	0.875
H_2	0.720	0.736	0.875
O	8.562	8.686	8.505
H_2O	10.0	10.158	10.255
Ti_3	12.0	11.85	11.787
Q_{Total}	22.0	22.0	22.0

Table III.4 Results for the unstretched H_2O on Ti_3. The 3 d electrons are assigned to the valence orbitals.

	H_2O & Clean Surface	OH = 1.8089 a.u.	OH = 2.4 a.u.	OH = 3 a.u.	OH = ∞	
E_{SCF}	-85.522	-85.505	-85.533	-85.544	-85.583	
E_B	———	-0.017	+0.011	+0.022	+0.061	
ΔE_{CI}	-0.125	-0.073	-0.068	-0.071	-0.111	
E_{Total}	-85.647	-85.578	-85.601	-85.615	-85.694	
E_B	———	-0.069	-0.046	-0.032	+0.047	(29.4 K cal/mol)
Mulliken population						
H_1	0.720	0.736	0.725	0.69	0.63	
H_2	0.720	0.736	1.237	1.151	1.0	
O	8.562	8.686	8.877	8.959	9.127	
H_2O	10.0	10.158	10.839	10.8	10.757	
Ti_3	12.0 (7.9d, 4.1s)	11.85	11.162	11.192	11.304	(7d, 4.3s)
Q_{Total}	22.0	22.0	22.0	22	22.0	

Table III.5 Results for the stretched case of H_2O on Ti. The 3 d electrons are assigned to the valence orbitals. The molecule is at 3 a.u. above the 3-fold site.

	H_2O & Clean Surface (infinite separation)	OH_1 = 2.4 a.u.	OH_1 = 3 a.u.	OH_1 = ∞
E_{SCF} (a.u.)	-85.522	-85.480*	-85.462*	-85.349*
E_B (a.u.)	———	-0.042	-0.06	-0.173

Table III.6 Results for the stretched OH_1 case. The 3 d electrons are assigned to the valence orbitals.

*H_2 is assumed to be at infinity and O is at 3 a.u. above the 3-fold site.

III.7.2.2 H_2O and the Lattice Have Common Plane

Here we consider the case in which H_2O and the Ti_3 lattice have a common plane. This geometry resembles what is called adsorption on step edges, that is the adsorbed molecule is very close to one or very few atoms and far away from the remainder of the lattice. The oxygen atom was set at 3 a.u. from atom 1 (see Fig. III.4a) and the calculation was done on the SCF level by stretching one of the OH bonds till complete dissociation occured. The results in table III.7 shows that the binding energy is always negative (unbound state) with the case in which H_2O dissociates into OH and H being the least unbound (binding energy is -0.10 a.u.). This pathway shows a resistance to the O-H stretch and consequently the calculations were not pursued further.

	H_2O & Clean Surface	OH = 1.8089	OH = 2.4 a.u.	OH = 3 a.u.	OH = ∞
E_{SCF} (a.u.)	-85.522	-85.382	-85.371	-85.397	-85.420
E_B (a.u.)	———	-0.140	-0.151	-0.125	-0.102

Table III.7 Results for the case where the H_2O and the Ti_3 have a common plane. The 3 d electrons are assigned to valence orbitals.

III.8 Potential Energy and Activation Barrier for H_2O on Ti_3

Our previous results have shown that by assigning the three 3d electrons to the valence orbitals, molecular H_2O is not bound to the Ti_3 surface when the lower end of the molecule (the oxygen atom) is at 3 a.u. above the 3-fold site (Table III.5). In order to find the potential energy curve a calculation for the total energy as the molecule approaches the lattice from infinity has to be carried out. The results are shown in table III.8 and are represented on the graph of Fig. III.5. As can be seen, all points fall on a smooth repulsive curve indicating a substantial barrier for molecular H_2O as it approaches the surface. However, dissociated H_2O into OH and H is proven to be bound to the surface. This tells us that there is an activation barrier for dissociation. Finding the activation barrier requires extra computations. These calculations are done by putting the molecule with its oxygen atom at 3.5 a.u. above the three-fold site and stretching the OH bond. The results are shown in table III.9. The binding energy for the dissociated case is -0.76 eV, which means an unbound state. By combining the results of tables III.5, III.8 and III.9, a potential energy curve as the molecule approaches and dissociates is shown in Fig. III.6. The maximum extent to which the intermediate configurations possess a greater energy than that of the separated systems is the activation energy. This value from the graph is 1.5 eV (34.5 K cal/mol).

Another calculation was done with the H_2O molecule at 4 a.u. above the three-fold site. The results is shown in table III.10. The dissociated case of H_2O into OH and H is very close to being bound (binding energy is -0.006 a.u.), and again there is $3\underline{d} \rightarrow 4\underline{s}$ charge promotion.

In most of our calculation for the adsorption and the dissociation of H_2O on Ti_3, we considered the geometries in which the H_2O molecular plane is perpendicular to the lattice plane. This means that the two hydrogen atoms are at their greatest distance from the surface. This choice is partly justified by the fact that in our two calculations in which the hydrogen atoms were pointing down toward the lattice the results were highly repulsive (Table III.2, III.4). This is also confirmed by the fact that in all dissociated cases, both the lattice and the hydrogen have gained a net positive change, and so they prefer to stay as far apart as possible. Although we do not completely rule out the possibility of a bound state for tilted geometry, it is highly improbable. Another point is that in the UPS experiment[32], the detection of high H^+ signal was attributed to the existence of OH perpendicular to the surface.

H_2O at	infinity	5 a.u.	4 a.u.	3.5 a.u.	3 a.u.
Total Energy (a.u.)	-85.647	-85.619	-85.603	-85.595	-85.578
Binding Energy (a.u.)	———	-0.028 (-0.76 eV)	-0.044 (-1.20 eV)	-0.052 (-1.41 eV)	-0.069 (-1.88 eV)

Table III.8 Total energy and binding energy for molecular H_2O on Ti_3 as the molecule approaches the surface from infinity

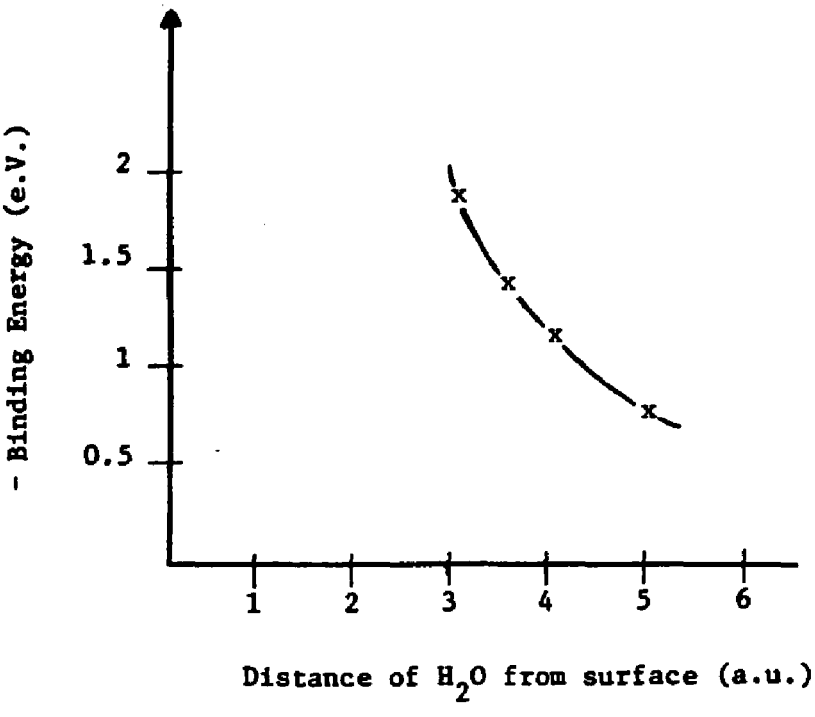

Figure III.5 Repulsive potential energy curve of H_2O - Ti_3 as a function of perpendicular distance of molecular H_2O from the surface

	H_2O & Clean Surface	OH = 1.8 a.u.	OH=2.4 a.u.	OH = 3 a.u.	OH = 3.5 a.u.	OH = ∞
Total Energy (a.u.)	-85.647	-85.594	-85.593	-85.612	-85.625	-85.619
Binding Energy (a.u.)	———	-0.053	-0.054	-0.035	-0.022	-0.028
		(-1.44 eV)	(-1.47 eV)	(-0.95 eV)	(-0.60 eV)	(-0.76 eV)

Table III.9 Total energy and binding energy when H_2O is at 3.5 a.u. above the 3-fold site

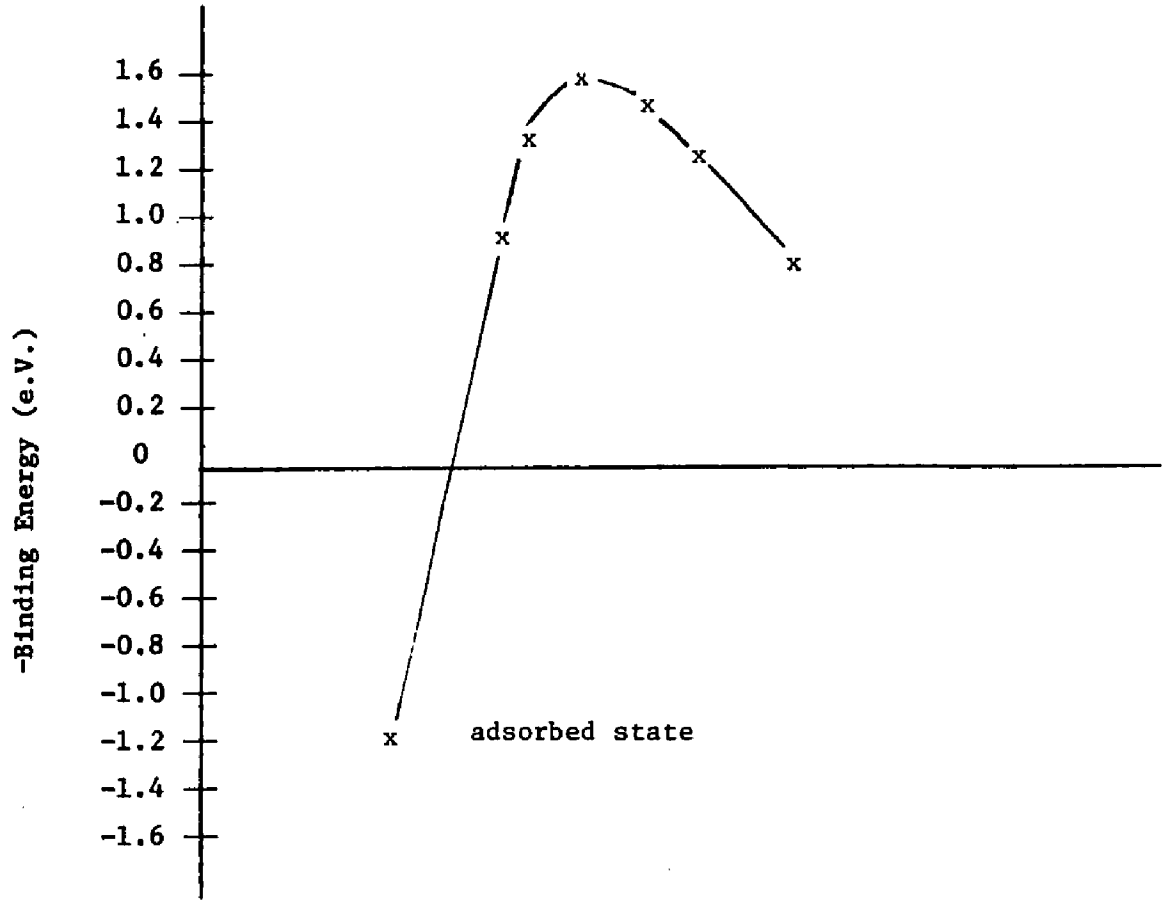

Figure III.6 Change in potential energy during adsorption and dissociation of H_2O on Ti_3 system

	H_2O & Clean Surface	OH = 1.8089 a.u.	OH = 2.4 a.u.	OH = 3 a.u.	OH = ∞
E_{SCF}	-85.522	-85.506	-85.517	-85.501	-85.519
E_B	———	-0.016	-0.005	-0.021	-0.003
ΔE (CI)	-0.125	-0.096	-0.088	-0.079	-0.122
E_{Total}	-85.647	-85.602	-85.605	-85.580	-85.641
E_B	———	-0.045	-0.042	-0.067	-0.006
Mulliken population					
H_1	0.720	0.705	0.705	0.722	0.702
H_2	0.720	0.705	1.302	1.185	1.0
O	8.562	8.649	8.863	8.953	9.136
H_2O	10.0	10.059	10.87	10.86	10.838
Ti_3	12.0 (7.9d, 4.1s)	11.9 (8d, 3.9s)	11.13(7.11d, 4.02s)	11.14 (7.31d, 3.83s)	11.164 (6.9d, 4.3s)
Q_{Total}	22.0	22.0	22.0	22.0	22.0

Table III.10 Results for the stretched case of H_2O on Ti_3. The 3d electrons are assigned to the valence orbitals. The molecule is at 4 a.u. above the 3-fold site.

III.9 The Seven Atom Cluster Calculation (Ti_7 - H_2O)

III.9.1 Introduction

In the previous section we have seen that the 3d electrons play a role the dissociation of water molecule on Ti_3. These results suggests that the 3d electrons should be treated as valence electrons in the chemisorption of H_2O on Ti_7. Since the number of two electron integrals increases as $\sim\frac{1}{8}\ n^4$, where n is the number of basis functions, two steps are taken to reduce the number of basis functions: (i) The 3d electrons on atoms 4 and 5 (Fig. III.2) are assigned to the core, thus reducing the number of basis functions by ten (ii). Of the 5d functions on each of atoms 1, 2, 3, 6 and 7 only the three functions which minimizes the total energy of Ti_7 are considered. The valence basis functions on atoms 4 and 5 are 4s and 4s' and on atoms 1, 2, 3, 6 and 7 are $3d_{xy}$, $3d_{xz}$, $3d_{y^2-z^2}$, 4s and 4s'. The lattice contributes 22 valence electrons and the water molecule contributes its 10 electrons to a total of 32 valence electrons. The reamining electrons are assigned to the core and contribute only an electrostatic potential. A unitary localization transformation was carried out following the SCF procedure using all the water molecule basis orbitals and the valence basis orbitals of the Ti atoms near the adsorption region to define the localization site. This procedure limits the CI to a tractable subspace of localized electrons and at the same time incorporates the delocalized character of the 4s bond into the local description. The purpose of the CI is twofold: to introduce electronic correlation in the description of adsorbate surface bonding and to permit further variation in the coupling of the d electrons in the local bonding region.

III.9.2 Computation

Our calculations on the chemisorption of H_2O on Ti_3 has given us some important information:

(i) the 3d electrons play a limited role in the dissociation of H_2O on Ti_3.

(ii) the unstretched geometry of H_2O is energetically unfavorable and only by stretching one of the O-H bonds can chemisorption of H_2O occur.

(iii) the 3d electrons tend to be singly occupied, a trial to doubly occupy them sends the total energy up. Based on this information, three different adsorption sites are considered and listed below for H_2O above the Ti_7 surface.

A. H_2O at 3 a.u. above the 3 fold-site created by atoms 3, 6 and 7.

B. H_2O at 3 a.u. above the bridge site midway between atoms 3 and 5.

C. H_2O at 3 a.u. above atom 3 (atop atom).

All the calculations are performed, unless otherwise stated, with the H_2O molecular plane perpendicular to the lattice plane.

The results of calculation A is shown in table III.11. Again, molecular H_2O is unbound (binding energy is -0.41 a.u.). However by stretching the O-H bond the energy goes down, and at complete dissociation of H_2O into H and OH, the energy is lower than the sum of the separated system energy by 0.045 a.u. (28.2 K cal/mol). This value for the binding energy is almost the same as the binding energy for the dissociated H_2O on Ti_3 (29.1 K cal/mol). One noticable difference is that the number

of d electrons for the separated system (14.5 e) remains the same as for the dissociated case (14.5 e), and all the 0.8 electron transfer to the adsorbate are taken from the s electrons. This is probably because more s electrons are available in the present system than for the Ti_3 system, and it indicates the limited role for d electrons in bonding.

Table III.12 shows the results of calculation B and it follows the same general trend. Molecular H_2O is unbound and by stretching the OH bond to 2.4 a.u. the system is bound and at complete dissociation the binding energy goes up to + 0.057 a.u. (35.7 K cal/mol) which is 7K cal/mol higher than calculation A. Again the number of d electrons remains the same for the separated systems and for the dissociated case. A trial is made to completely dissociate H_2O into 2H and O; this is done by stretching the other OH bond till complete dissociation occurs. The results in table III.13 show that stretching the other OH bond causes the energy to go up and at complete dissociation the binding energy is -0.12 a.u. (unbound). This result is the same as the completely dissociated H_2O on Ti_3 (Table III.6) and it indicates that the completely dissociated H_2O is energetically unfavorable. Results of calculation C (a top atom case) is shown in Table III.14. Here the molecular H_2O is highly unbound to the surface (binding energy is -0.208 a.u.) and by stretching the OH bond, the energy goes down but not enough to have a bound state.

	H_2O and Clean Surface	OH = 1.8089 a.u.	OH = 2.2 a.u.	OH = 2.6 a.u.	OH = 3 2.u.	OH = ∞
E_{SCF} (a.u.)	-92.046 (-75.989 - 16.075)	-92.028	-92.062	-92.067	-92.072	-92.096
ΔE_{CI}	-0.128	-0.105	-0.100	-0.098	-0.100	-0.123
Total Energy	-92.174	-92.133	-92.162	-92.165	-92.172	-92.219
Binding Energy	———	-0.041	-0.012	-0.009	-0.002	+0.045 (28.2 K cal/mol)
Mulliken Population						
H_1	0.720	0.789	0,929	0.781	0.706	0.734
H_2	0.720	0.789	1.25	1.309	1.3	1.0
O	8.562	8.668	8.696	8.776	8.848	9.126
H_2O	10.0	10.246	10.875	10.866	10.854	10.86
Ti_7	22.0 (14.5d, 7.5s)	21.76 (14.6d, 7.16s)	21.14 (14.5d, 6.6s)	21.13 (14.5d, 6.62s)	21.15(14.52d, 6.63s)	21.23 (14.5d, 6.7s)
Q_{Total}	32.0	32.0	32.0	32.0	32.0	32.0

Table III.11 Results for the dissociated case of H_2O on the 3-fold site of Ti_7.

	H_2O & Clean Surface	OH = 1.8 a.u.	OH = 2.4 a.u.	OH = 3 2 a.u.	OH = ∞
E_{SCF}	-92.046	-92.067	-92.094	-92.109	-92.099
ΔE (C.I.)	-0.127	-0.100	-0.100	-0.104	-0.131
Total Energy	-92.173	-92.167	-92.194	-92.213	-92.230
Binding Energy	———	-0.006	+0.021	+0.04	+0.057 (35.7 K cal/mole)
Mulliken Population					
H_1	0.72	0.663	0.604	0.615	0.819
H_2	0.72	1.467	1.32	1.224	1.0
O	8.562	8.627	8.878	8.972	9.034
H_2O	10.0	10.757	10.802	10.811	10.853
Ti_7	22.0 (14.5d, 7.5s)	21.25 (14.55d, 6.69s)	21.2 (14.55d, 6.66s)	21.19 (14.54d, 6.65s)	21.15 (14.53d, 6.62s)
Q_{Total}	32.0	32.0	32.0		32.0

Table III.12 Results for the dissociated case of H_2O on the bridge site of Ti_7.

	H_2O & Clean Surface	$OH_2 = \infty$ OH_1 = 3 a.u.	$OH_2 = \infty$ $OH_1 = \infty$
E_{SCF}	-92.046	-91.964	-91.926
E_B	———	-0.082	-0.12

Table III.13 Results for the completely dissociated case for H_2O above the bridge site of Ti_7

	H_2O & Clean Surface	OH = 1.8089 a.u.	OH = 2.4 a.u.	OH = 3 a.u.	OH = ∞
E_{SCF} (a.u.)	-92.045	-91.838	-91.933	-91.952	-91.968
E_B (a.u.)	———	-0.208	-0.113	-0.094	-0.078

Table III.14 Results for the dissociated case of H_2O above the a top atom of Ti_7

CHAPTER IV

CHEMISORPTION ON Ti_{28} AND CONCLUSION

IV.1 Chemisorption on Ti_{28}

IV.1.1 Introduction

In the present calculation we are considering the chemisorption of H_2O on the close packed Ti_{28} two layer cluster. The surface layer has sixteen atoms and the second layer has twelve atoms. The geometry used is shown in Fig. IV.1. The valence basis functions were chosen to be 4 s on all the twenty eight atoms with additional 4s' functions on the seven atom "surface" hexagonal cluster defined in Fig. IV.1. The 3 d electrons were assigned to the core and contribute only an electrostatic potential. The reason for this choice came after analyzing the results of the chemisorption of H_2O on Ti_7. These results have shown that there was no charge transfer from the 3 d electrons to the adsorbate and all the charge transfer came from the 4 s electrons. The total number of valence basis functions used in the present system is 49 (35 on Ti_{28} + 14 on H_2O). Each Ti atom contributes one 4 s valence electron and the water molecule contributes all of its 10 electrons to a total of 38 valence electrons. The core potentials and Ti basis functions are given in the appendix. The unitary localization transformation was carried out using the H_2O orbitals and the neighboring Ti atoms on the surface to define the localization site. This procedure limits the CI to a tractable subspace of localized electrons and at the same time incorporates the delocalized character of the 4 s band into the local description.

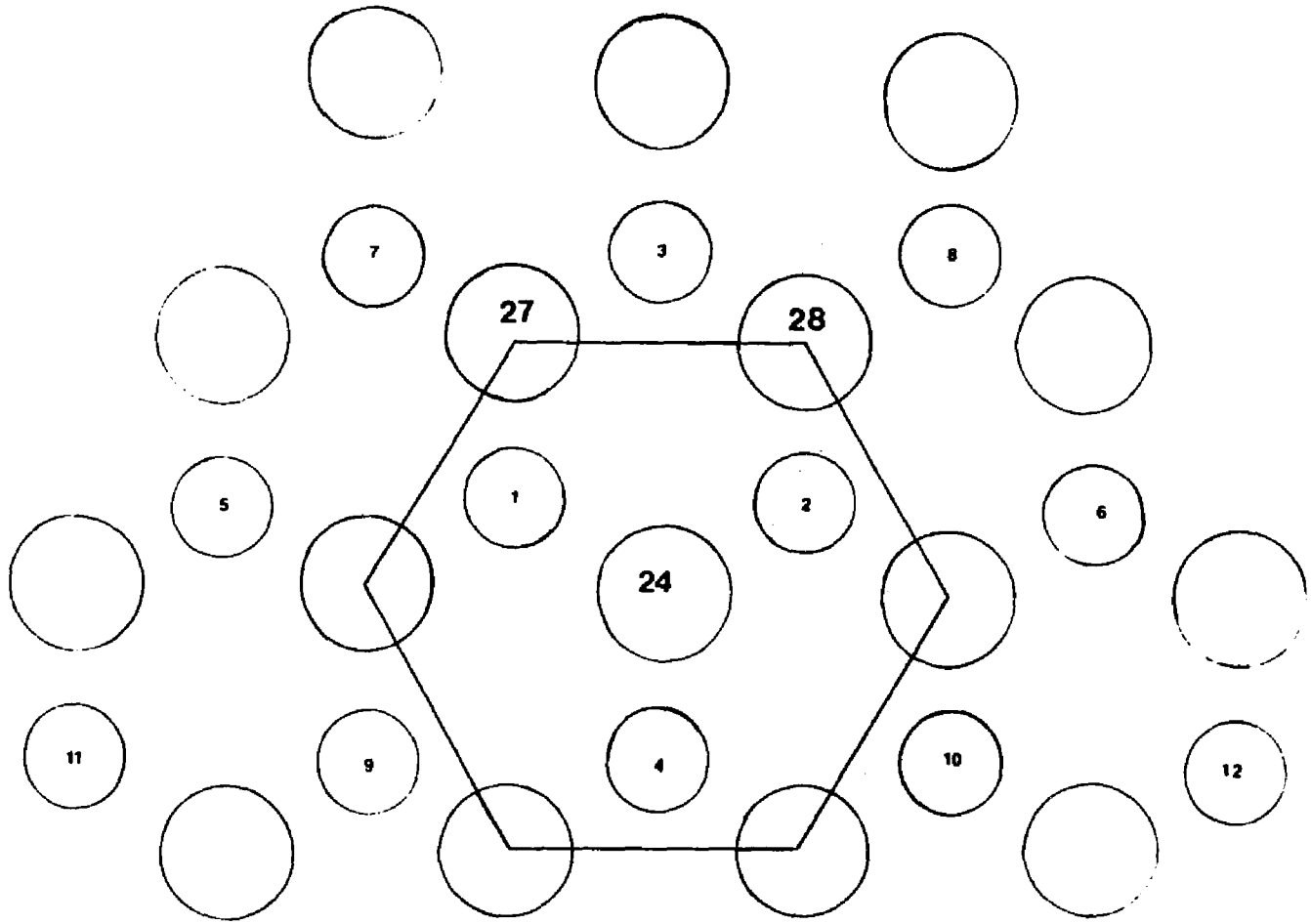

Ti_{28} CLUSTER (Atoms 1→12 Are Second Layer)

IV.1.2 Computation

The calculation was done by putting the water molecule at 3 a.u. above the 3-fold site defined by atoms 24, 27 and 28 in Fig. IV.1 with the molecular plane perpendicular to the lattice plane. The results are shown in Table IV.1 for both molecular, stretched and dissociated case of H_2O above the Ti_{28} lattice. Unlike the case of Ti_3 and Ti_7 molecular H_2O was found to be bound to the surface with binding energy of + 0.019 a.u., and by stretching one of the OH bonds to 2.6 a.u. the binding energy increases to + .026 a.u. and H_2O dissociated into OH and H was found to be the most bound with binding energy of +0.053 a.u. (33.2 K cal/mol). The charge transfer to the H_2O molecule was found to increase from .03 e for the molecular case to 0.77 e for the dissociated case. The binding energt for the present dissociated system, 33.2 K cal/mol, is slightly higher than the binding energy for the dissociated H_2O on the 3-fold site of Ti_3 for the case where the 3 d electrons were assigned to the core, 25 K cal/mol (Table III.3). However the charge transfer from the lattice to the adsorbate was found to be the same, 0.77 e.

	H_2O + Clean Surface	OH = 1.8089 a.u.	OH = 2.6 a.u.	OH = ∞
E_{SCF}	-78.378	-78.430	-78.392	-78.429
ΔE_{CI}	-0.138	-0.105	-0.150	-0.140
E_T (a.u.)	-78.516	-78.535	-78.542	-78.569
E_B (a.u.)		+0.019	+0.026	+0.053 (33.2 K cal/mol)
Mulliken Population (a.u.)				
H_1	0.72	0.693	0.621	0.663
H_2	0.72	0.693	1.014	1.0
O	8.562	8.645	8.869	9.108
H_2O	10.0	10.031	10.504	10.771
Ti_{28}	28.0	27.969	27.5	27.229
Q_{Total}	38.0	38.0	38.0	38.0

Table IV.1 Results for the stretched case of H_2O on Ti_{28}. The 3 d electrons are assigned to the core.

IV Conclusion

The self consistent field method followed by the configuration interaction method to account for electron correlation effects were used to study the Ti_3-H_2O, Ti_7-H_2O and Ti_{28}-H_2O interactions. The small cluster calculations (Ti_3-H_2O) gave us some important information about the nature of this interaction. By treating the 3 d electron as core electrons molecular H_2O was found to be almost bound with the two hydrogen atoms pointing away from the lattice and a 0.12 e charge transfer from the lattice to the molecular H_2O. However by stretching one of the OH bonds, the binding energy was found to increases from zero to + 0.040 a.u. (25 K cal/mol) at complete dissociation of H_2O into OH and H and also the charge transfer went up to 0.77e (Table III.3). Another calculation was done on the Ti_3-H_2O system by considering the 3 d electrons as valence electrons Here molecular H_2O was found to be highly repulsive with binding energy of -0.69 a.u. (-43 K cal/mol) and by stretching one of the OH bonds the binding energy increases to + 0.47 a.u. (29.4 K cal/mol) at complete dissociation of H_2O into OH and H (Tbale III.5). The 29.4 K cal/mol binding energy is about 15% higher than the 25 K cal/mol binding energy for the case where the 3 d electrons were assigned to the core which indicates a limited role for the 3 d electrons in bonding. However the amount of charge transfer to the adsorbate from the lattice is the same (0.77 e). From the later case, all the charge transfer came from the 3 d electrons which seem to contradict the limited role of the 3 d electrons in bonding. The explanation is that the 3 d electrons were proven to play an important role in bonding between surface Ti atoms and in the present system there are only a few of them available so they donate the extra

charge to the adsorbate.

As mentioned above there was no activation barrier by treating the 3 d electrons as core electrons. However, by treating the 3 d electrons as valence electrons, molecular H_2O was found to be highly repulsive and the dissociated H_2O (OH + H) was bound which indicate the existence of an activation barrier to dissociation. Finding the potential energy change during adsorption and dissociation required an extra computations which was done at lattice-adsorbate distance of 5, 4 and 3.5 a.u. The outcome of these compurations is shown in Fig. III.5 and Fig. III.6, and from the last curve the activation barrier was found to be 1.5 eV (34.5 K cal/mol).

A trial was made to completely dissociate H_2O into O and 2H and as shown in Table III.6, the energy of this state is 0.173 a.u. above that of the separated systems which indicate a highly repulsive state and that atomic oxygen does not exist on the surface. The conclusion of our computations of Ti_3-H_2O is that OH and H do exist on the surface which is agreement with the UPS experiment of Stockbaur et al[32] and that atomic oxygen derived from H_2O does not exist on the surface which contradicts the experiment.

The Ti_7-H_2O calculations was performed at lattice-adsorbate distance of 3 a.u. and the 3 d electrons were treated as valence electrons. Three adsorption sites were considered, the 3-fold site, bridge site and the atop-atom site. The results of the 3-fold site is shown in Table III.11. Again molecular H_2O was found to be repulsive with binding energy of -.041 a.u. (-25.7 K cal/mol). However, this state is less repulsive than the case of Ti_3 in which the binding energy was found to be -0.069 a.u. (-43 K cal/mol). By stretching one of the OH bonds, the energy was

found to go down and at the dissociated state of H_2O into OH and H, the energy was lower than that of the seperated systems by 0.045 a.u. which indicate a bound state of binding energy .045 a.u. (28.2 K cal/mol). This value of binding energy is almostthe same as the case of Ti_3. In contrast to the Ti_3 results, all the charge transfer from the lattice to the adsorbate came from the 4 s electrons and as explained in the text this is probably because there are more 4 s electrons available in the Ti_7 than in Ti_3 and in Ti_7 there are more atoms available for the 3 d electrons to participate in bonding of the Ti atoms with each other and not with the adsorbate.

The bridge site calculations have shown that molecular H_2O is very close to being bound with binding energy of -.006 a.u. (-3.7 K cal/mol) and the dissociated case of H_2O into OH and H was strongly bound with binding energy of +0.57 (35.7 K cal/mol). A trial was made to completely dissociate H_2O into O and 2H on this bridge site and as shown in Table III.13 this completely dissociated case was found to have an energy of 0.12 a.u. (75 K cal/mol) higher than that of the separated systems which indicates a highly repulsive state and that atomic oxygen from H_2O does not exist on the surface. The atop atom calculations have shown that molecular H_2O is very highly repulsive with binding energy of -0.208 a.u. (-130.3 K cal/mol) and that the dissociated H_2O into OH and H is still repulsive with binding energy of -.078 a.u. (-49.5 K cal/mol). Concluding our results on Ti_7 we can say that molecular H_2O is less repulsive than the case of Ti_3 and that the dissociated H_2O into OH and H is more bound specailly on the bridge site of Ti_7.

The Ti_{28}-H_2O computations was performed by treating the 3 $\underline{d}$ electrons as core electrons and both molecular and dissociated H_2O into OH and H were found to be bound. Molecular H_2O was found to have a binding energy of 0.019 a.u. (12 K cal/mol) and the dissociated one had a binding energy of + .053 a.u. (33.2 K cal/mol). Comparing the Ti_{28} and Ti_3 calculations for the case where the 3 $\underline{d}$ electrons were assigned to the core we can conclude that by increasing the cluster size from 3 atoms to 28 atoms, both molecular and dissociated H_2O tend to be more bound. However the amount of charge transfer from the lattice to the adsorbate was found to be the same for both cases (0.77 e).

In conclusion, we can say that the SCF-CI method gives an accurate description of the total energy. Thus, it can determine the geometry of a chemisorbed system by finding the lowest possible energy among the possible geometries.

Appendix I

Valence Basis Orbitals

H 1s

Exponents	Coefficients
32.39346	0.03154
4.95977	0.22826
1.14780	1.0
.32585	2.47509

H 1s'

Exponents	Coefficients
0.10297	1.00

O 1s

290.8205	1.0
1424.0643	0.1344
4693.4485	0.0323

O 1s'

31.3166	1.00
12.8607	1.8781
4.6037	1.0838
76.2320	0.6261

O 2s

.9311	1.1526
9.7044	-0.1538

O 2s'

.2825	1.00

O 2p

46.2879	1.0
9.0369	15.7917
2.3606	84.9397
0.7031	202.777

O 2p'

0.212	1.00

Ti 4s

Exponents	Coefficients
129.000	-0.059465
7.890	0.245117
.716	-0.790125
.0774	0.58913632
.0328	1.369954

Ti 4s'

Exponents	Coefficient
129.000	-0.0409358
7.890	.1707074
.716	-0.6150853
.0774	2.3629359
.0328	-2.0346547

Ti 3d

Exponents	Coefficients
5.05771	0.2552
1.13670	0.51483
0.25896	0.46154

Appendix II

Core Potentials and Core Basis Orbitals

Starting with the full electrostatic Hamiltonian of the adsorbate lattice system for N' electrons and Q nuclei

$$H = \sum_{i}^{N'} -\frac{1}{2}\nabla_i^2 - \sum_{i}^{N'}\sum_{k}^{Q}\frac{Z_k}{r_{ki}} + \sum_{i<j}^{N'}\frac{1}{r_{ij}} \; ;$$

Localization of the core electrons into a set of atomic core orbitals $\{Q_M\}$ reduces the dimensionality of the problem to N valence electrons in the coulomb and exchange field of the core. Gaussian basis functions are used to expand the single-particle orbitals from which SCF and CI functions are constructed. The core electron density matrix $\gamma_c(1, 2) = \sum_M Q_M(1)\, Q_M(2)$ and the core electron density $P_c(1) = \gamma_c(1, 1)$ are likewise expanded in terms of Gaussians. The Hamiltonian for the valence electrons then becomes

$$H = \sum_{i} h_i + \sum_{i<j}\frac{1}{r_{ij}},$$

where

$$\langle f_i|h_1|f_j\rangle = \left\langle f_i\left|-\tfrac{1}{2}\nabla_i^2 - \sum_k \frac{Z_k}{r_{k1}}\right|f_j\right\rangle + \langle f_i(1)f_j(1)|r_{12}^{-1}|\rho_c(2)\rangle - \langle f_i(1)f_j(2)|r_{12}^{-1}|\gamma_c(1,2)\rangle.$$

Spin orbitals for the valence electrons f_i' are orthogonalized to the core Spin orbitals for the valence electrons f_i' are orthogonalized to the core orbitals, $f_i' = f_i - \Sigma_M \langle f_i/Q_M\rangle\, Q_M$.

Core-valence overlap considerations are usually handled by constructing a pseudopotential for the valence electrons. In the present work, we proceed along somewhat different lines. First, the valence basis functions of a given atom are rigorously orthogonalized to the core orbitals of that atom using a simple auxiliary basis. For example, let u be a 4s basis function not orthogonal to the core of s orbitals. Gram-Schmidt orthogonalization gives

$$|u'\rangle = |u\rangle - \sum_{k=1}^{3} \langle u|ks\rangle |ks\rangle .$$

Alternatively, let functions s_1, s_2, s_3 be approximations to the 1s, 2s and 3s orbitals; it is possible to define

$$|u'\rangle = |u\rangle - \sum_{k=1}^{3} \lambda_k |s_k\rangle ,$$

with linear coefficients chosen such that <ks/u'> = 0 for all k. The significant point from atomic calculations is that an accurate representation of valence orbitals of transition metals can be found using simple Gaussian expansions for the auxiliary basis $\{s_k\}$.

The effect of orthogonalizing valence basis functions to their respective core orbitals is to eliminate all one-center overlaps. For nearest neighbor Ti atoms at an internuclear distance corresponding to the bulk value, the largest core-valence overlap is 0.09 for $< 4s_A/4s_B >$. These non-zero overlaps are not negligible, but their smallness permits certain approximations of the energy expression as described below.

Consider the determinantal wave function

$$\psi = (\text{norm})\mathcal{A}(Q_1 Q_2 \cdots Q_c \chi_1 \chi_2 \cdots \chi_N),$$

where Q_k and χ_k are spin orbitals for the core and valence electrons respectively, after an orthogonalizing linear transformation

$$\psi = (\text{norm})' \ (Q_1 Q_2 \ \cdots \ Q_c \chi_1' \chi_2' \ \cdots \ \chi_N'),$$

where $\chi_i' = \chi_i - \Sigma_M < \chi_i / Q_M > Q_M$, $< Q_i / Q_j > = \delta_{ij}$ (by assumption), and $< \chi_i' / \chi_j' > = \delta_{ij}$, $< \chi_i' / Q_j > = 0$ (by construction). Defining

$$\gamma'(1,2) = \sum_j \chi_j'(1)\chi_j'(2), \quad \rho'(1) = \gamma'(1,1),$$

$$\gamma_c(1,2) = \sum_j Q_j(1) Q_j(2), \quad \rho_c(1) = \gamma_c(1,2)$$

permits expression of the total energy as

$$E = <\psi|H|\psi> = E_{core} + \sum_i <\chi_i'|h|\chi_i'> + (\rho'(1)|r_{12}^{-1}|\ \tfrac{1}{2}\rho'(2) +$$

$$\rho_c(2)) - <\gamma'(1,2)|r_{12}^{-1}|\ \tfrac{1}{2}\gamma'(1,2) + \gamma_c(1,2)>.$$

Defining $\gamma(1,2) = \Sigma_j \chi_j(1)\chi_j(2)$, $\rho(1) = \gamma(1,1)$ gives

$$E = E_{core} + \sum_i <\chi_i|h|\chi_i> + (\rho|r_{12}^{-1}|\tfrac{1}{2}\rho + \rho_c) - <\gamma|r_{12}^{-1}|\tfrac{1}{2}\gamma + \gamma_c>$$

$$+ \sum_i (<\chi_i'|h|\chi_i'> - <\chi_i|h|\chi_i>) + (\rho' - \rho|r_{12}^{-1}|\tfrac{1}{2}\rho + \tfrac{1}{2}\rho' + \rho_c>$$

$$- <\gamma' - \gamma|r_{12}^{-1}|\ \tfrac{1}{2}\gamma + \tfrac{1}{2}\gamma' + \gamma_c>$$

Writing $\rho' - \rho = \Sigma_M(\rho' - \rho)_M$ and $\gamma' - \gamma = \Sigma_M(\gamma' - \gamma)_M$ to show the contributions from individual core orbitals and introducing atom densitites $\bar{\rho}_M$, $\bar{\gamma}_M$,

$$E - E_{core} = \sum_i \langle \chi_i | h | \chi_i \rangle + (\rho | r_{12}^{-1} | \tfrac{1}{2}\rho + \rho_c) - (\gamma | r_{12}^{-1} | \tfrac{1}{2}\gamma + \gamma_c) \qquad \text{A}$$

$$+ \sum_i [\langle \chi_i' | -\tfrac{1}{2}\nabla^2 | \chi_i' \rangle - \langle \chi_i | -\tfrac{1}{2}\nabla^2 | \chi_i \rangle] + \sum_M \left((\rho' - \rho)_M \left| \frac{-Z_M}{r_M} \right. \right) + \sum_M ((\rho' - \rho)_M | r_{12}^{-1} | \bar{\rho}_M) - \sum_M ((\gamma' - \gamma)_M | r_{12}^{-1} | \bar{\gamma}_M) \qquad \text{B}$$

$$+ \sum_M \left[((\rho' - \rho)_M | r_{12}^{-1} | \tfrac{1}{2}\rho' + \tfrac{1}{2}\rho + \rho_c - \bar{\rho}_M) + \left((\rho' - \rho)_M \left| \sum_N^{\neq M} - \frac{Z_N}{r_N} \right. \right) \right] \qquad \text{C}$$

$$- \sum_M ((\gamma' - \gamma)_M | r_{12}^{-1} | \tfrac{1}{2}\gamma' + \tfrac{1}{2}\gamma + \gamma_c - \bar{\gamma}_M). \qquad \text{D}$$

The above energy expression is still exact. Term A requires only interactions of the valence orbital basis for its evaluation. Term B requires the reproduction of the core valence overlap $\langle \chi_i / Q_M \rangle$. Terms B and C require approximation but neither term is large in magnitude.

Core Orbitals for Ti

1s (-182.9)		2s (-20.93)		3s (-2.54)	
Exponent	Coefficient	Exponent	Coefficient	Exponent	Coefficient
48680.0	.00152722	1638.02	-.02279808	1638.02	.00815052
7144.04	.012192197	465.527	-.06335135	465.527	.0229929
1638.02	.059259316	152.394	-.18580639	152.394	.068588725
465.527	.206435454	54.0349	-.23201237	54.0349	.092268487
152.394	.438405276	13.2356	0.40920074	13.2356	-.212066571
54.0349	.393362514	5.47417	0.68304667	5.47417	-.532268
13.2356	.05202095	1.3887	.07896798	1.3887	.517857648
5.47417	-0.01588225	.58837	-.01877786	.58337	.70292033
1.3887	.00534742	.080663	.00425277	.080663	.03119005
0.58337	-.00224237	.032828	-.00212617	.032828	-.01235507

2p (-17.41)		3p (-1.53)	
284.565	.4282	284.565	-0.150737
66.9	2.7111	66.9	-.956112
20.7458	7.55035	20.7458	-3.003233
7.1333	8.16664	7.1333	-2.6560715
1.8714	1.24258	1.8714	8.585336
0.596298	-.186587	0.596298	10.28746

Core Potential

No free d electrons		Free three 3d electrons	
1.328	-13.67816	1.328	-13.67816
21.28	-.63201	21.28	-.63201
497.0	-.019689	497.0	-.019689
.45	-7.6612		

BIBLIOGRAPHY

1. P.S. Bagus and M. Seel, Phys. Rev. B23. 2065 (1981).

2. W.A. Goddard et al., J. Vac. Sci. Technology, 416 (1977).

3. C.R. Fischer, L.A. Burke and J.L. Whitten, Phys. Rev. Lett. 49, 344 (1982).

4. R. McWeeny: In Molecular Orbitals In Chemistry, Physics and Biology, ed. by P.O. Löwdin, B. Pullman (Academic Press, New York, 1964).

5. J.C. Slater, "The Self Consistent Field for Molecules and Solids," Vol. 4, McGraw Hill (1974).

6. P. Hohenberg, W. Kohn, Phys. Rev. 136, B864 (1964).

7. C.C.J. Roothaan, Revs. Modern Phys. 23, 69 (1951).

8. C.C.J. Roothaan, Revs. Modern Phys. 32, 179 (1960).

9. J.L. Whitten, T.A. Pakkanen, Phys. Rev. B21, 4357 (1980).

10. C. Edmiston and K. Ruedenberg, Rev. Mod. Phys. 35. 457 (1963).

11. J.L. Whitten and M. Hackmeyer, J. Chem. Phys. 51, 5584 (1969).

12. S. Brunauer, K.S. Love, and R.G. Keenan, J. Am. Chem. Soc. 64, 751 (1942).

13. C.J. Davisson and L.H. Germer, Phys. Rev. 30, 705 (1927).

14. P.J. Estrup and E.G. McRae, Surface Sci. 25, 1 (1971).

15. J.E. Houston and R.L. Park, Surface Sci. 21, 209 (1970).

16. G.A. Somorjai, Principles of Surface Chemistry, Prentice-Hall, Inc. (1972).

17. S.J. Atkinson, C.R. Brundle, and M.W. Roberts, Discuss. Faraday Soc. 58, 62 (1974).

18. G.B. Fisher and J.L. Gland, Surf. Sci. 94, 446 (1980); G.B. Fisher and B.A. Sexton, Phys. Rev. Lett. 44, 683 (1980).

19. H. Ibach and S. Lehwald, Surf. Sci. 91, 187 (1980).

20. D.J. Dwyer, G.W. Simmons, and R.P. Wei, Surf. Sci 64, 617 (1977).

21. C. Benndrof, C. Nobl, M. Rusenberg and F. Thieme, Surf. Sci. III, 87 (1981).

22. R.A. Rosenberg, V. Rehn, V.O. Jones, A.K. Green, C.C. Parks, G. Loubriel, and R.H. Stulen, Chem. Phys. Lett. 80. 488 (1981).

23. F.P. Netzer and T.E. Madey, Phys. Rev. Lett. 47, 928 (1981).

24. K. Fujiwara, Surf. Sci. 108, 124 (1981).

25. D. Schmeisser, F.J. Himpsel, and G. Hollinger, Phys. Rev. B 27, 7813 (1983); D. Schmeisser, Surf. Sci. 137, 197 (1984).

26. H. Ibach, H. Wagner, and D. Bruchmann, Solid State Commun. 42 457 (1983).

27. H. Kobayashi, T. Kubota, M. Onchi, and M. Nishijma, Phys. Lett. 95A, 345 (1983); J.A. Schäfer, F. Stucki, D.J. Frankel, G.J. Lapeyre, and W. Göpel, J. Vac. Sci. Technol. B2, 359 (1984).

28. Y.J. Chabal, and S.B. Christman, Phys. Rev. B 29, 6974 (1984).

29. S. Anderson, C. Nyberg, and C.G. Tengstal, Chem. Phys. Lett. 104, 305 (1984).

30. J.E. Müller, and J. Harris, Phys. Rev. Lett. 53, 2493 (1984).

31. M.W. Ribarsky, W.D. Luedtke, and U. Landman, Phys. Rev. B 32, 1430 (1985).

32. R. Stockbauer, D.M. Hanson, S.A. Flodström, and T.E. Madey, Phys. Rev. B 26, 1885 (1982).

33. R. Stockbauer, D.M. Hanson, and T.E. Madey (unpublished).

34. P.J. Feibelman, D.R. Hamann, F.J. Himpsel, Phys. Rev. B 22, 1734 (1980).

35. D.M. Hanson, R. Stockbauer, and T.E. Madey, Phys. Rev. B 24, 5513 (1981).

36. S. Katsumara, and D.R. Lioyd, Chem. Phys. Lett. 45, 519 (1977).

37. C.R. Brundle and M.W. Roberts, Surf. Sci. 38, 234 (1973).

38. R. Stockbauer, D.M. Hanson, and T.E. Madey (unpublished).

39. L.C. Snyder and H. Basch, Molecular Wave Functions and Properties (John Wiley, 1972).

40. C.F. Melius, J.W. Moskowitz, A.P. Mortola, M.B. Baines, and M.A. Ratner, Surf. Sci. 59, 279 (1976).

41. A.B. Kunz, M.P. Guse, and R.J. Blint, J. Phys. B 8, L358 (1975).
R.J. Blint, A.B. Kunz, and M.P. Guse, Chem. Phys. Lett. 36, 191 (1975).
A.B. Kunz, M.P. Guse and R.J. Blint, Chem. Phys. Lett. 37, 512 (1976).
A.B. Kunz, M.P. Guse and R.J. Blint, Int. J. Quart. Chen. Synp. 10, 10, 283 (1976).
A.B. Kunz, M.P. Guse, and R.J. Blint, "Electrocatalysis on Non-Metallic Surfaces" (NBS Special Publication 455, 1976).
M.P. Guse, R.J. Blint and A.B. Kunz, Int. J. Quart. Chen. 11, 725 (1977).
M.P. Guse, Thesis, University of Illinois (1976) unpublished.

42. P. Cremaschi, and J.L. Whitten, Phys. Rev. Lett. 46. 1242 (1981).

43. R.P. Messmer, D.R. Salahub, K.H. Johnson, and C.Y. Yang, Chem. Phys. Lett. 51, 84 (1977).

44. C.R. Fischer, and J.L. Whitten, Phys. Rev. B 20, 1553 (1979).